NTNU
Norwegian University of
Science and Technology

Kinetics and Mechanism of Phase Transformations from Quartz to Cristobalite

Marthe Erdal Kjelstadli

Materials Technology
Submission date: June 2016
Supervisor: Halvard Tveit, IMTE
Co-supervisor: Eli Ringdalen, SINTEF

Norwegian University of Science and Technology
Department of Materials Science and Engineering

Preface

This report describes an investigation of the mechanisms and kinetics of the phase transformations from β-quartz to β-cristobalite during heating. The project is done as the evaluation basis for the course TMT4900 at the Norwegian University of Science and Technology, NTNU. The work was performed at the Department of Material Science and Engineering.

I would like to thank my supervisors, Prof. II Halvard Tveit and Dr. Eli Ringdalen at Sintef Materials and Chemistry for giving me the opportunity to write this project and I would like to thank Eli Ringdalen for helpful and greatly appreciated discussions and guidance. I would also like to thank research scientist Julian Tolchard for his very useful help and discussions regarding the XRD analysis, Ove Darrell for all the help with the heating experiments, Tone Anzjøn for helping with light microscopy and wettability experiments, Jonas Einang Gjøvik for helping with logging the experiments and Michal Ksiazek for the help with temperature simulations.

I would like to thank the SiManTi group for useful help and input and also for the fun and inspiring trips. Finally, I must give a huge thanks to Karin Fjeldstad Jusnes, Siri Marie Bø and Sofie Aursjø for all the support and insightful discussions.

Trondheim, June 2016

Marthe Erdal Kjelstadli

Abstract

The largely debated silica polymorphism has in this thesis been investigated for the transformation from β-quartz to β-cristobalite. It is done as a step in understanding and improve the furnace operations of the silicon process.

The goals of this thesis has been to describe the kinetics and the mechanism for phase transformations from β-quartz to β-cristobalite. This is done by:

- Identifying the phases and phase transformations of silica at temperatures of 1600°C and 1700°C.
- Investigating potential size effects between different sizes of particles of quartz after heating.
- Visually investigating quartz samples during and after heating.

Qz 29, which is a Faleq, has been investigated after heating to 1600°C and 1700°C in a rapid heating furnace and later analyzed with XRD. The amorphous phase has in the XRD analysis been quantified by the internal standard method. This method is found to be relatively accurate. In addition, has a sample been studied during heating to 1600°C in a wettability furnace. The volume expansion was also calculated during heating.

Quartz samples obtained from a furnace excavation has been investigated to study size effect in particles exposed to the environment of a silicon furnace.

It has been found that the transition to the amorphous phase is rapid, and the rate limiting factor for this transition seem to be the heat distribution in the particle. The further transition to β-cristobalite is slow and is for the transformation from β-quartz to β-cristobalite the rate limiting transformation.

A size effect is found for particles heated to 1700°C, but not in samples heated to 1600°C and samples from furnace excavation. It is therefore in this thesis concluded

that a size effect could be seen in samples exposed to a fast heating rate and high temperatures.

Sammendrag

Den mye omdiskuterte silikapolymorfismen har i denne rapporten blitt undersøkt for transformasjonen fra β-kvarts til β-kristobalitt. Dette er gjort som en del av å skape forståelse og forbedre ovnsdriften for silisiumproduksjon.

Målene for oppgaven har vært åbeskrive kinetikk og mekanisme for fasetransformasjoner fra β-kvarts og β-kristobalitt. Dette er gjort ved :

- Identifisere fasene og fasetransformasjonene i silika ved temperaturer på 1600°C og 1700°C.
- Undersøke potensielle størrelseseffekter mellom forskjellige partikkelstørrelser av kvarts ved oppvarming.
- Visuelt undersøke kvartsprøver under og etter oppvarming

Qz 29, som er av typen Faleq, har blitt undersøkt etter oppvarming til 1600°C og 1700°C i en hurtigovn og senere analysert med XRD. Amorf fase har i XRD-analysen blitt kvantifisert ved *internal standard*-metoden. Denne metoden er funnet til være relativt nøyaktig. I tillegg har en prøve blitt undersøkt under oppvarming til 1600°C i en fuktningsovn. Volumekspansjonen ble også kalkulert under oppvarming.

Kvartsprøver hentet ut fra en ovnsutgraving har blitt undersøkt for studere størrelseseffekten i partikler utsatt for forholdene i en silisiumovn.

Det er funnet at transformasjonen til amorf fase er hurtig, og at den hastighetsbegrensende faktoren for denne overgangen ser ut til være oppvarmingen av kvartspartikkelen. Den videre overgangen til β-kristobalitt er treg, og er for transformasjonen fra β-kvarts til β-kristobalitt den hastighetsbegrensende transformasjonen.

En størrelseseffekt er funnet for partiklene varmet til 1700°C, men ikke i prøver varmet til 1600°C og prøver fra ovnsutgravning. Det er derfor i denne oppgaven

konkludert med at størrelseseffekt kan sees i prøver utsatt for en rask oppvarming og høye temperaturer.

List of symbols

Kinetics

Symbol	Units	Description
A	m^2	Area
C_B	mol/m^3	Concentration of substance B
d	m	Actual diameter
d_0	m	Initial diameter
d_m	m	Mean diameter
D_B	m^2/s	Diffusivity of substance B
$\frac{dn}{dt}$	-	Reaction rate
$\langle \mathrm{d} \rangle$	m	Average particle size
$\langle D_v \rangle$	m^3	Volume-average domain size
ϵ	-	Void fraction
ΔG	J/mol	Gibbs energy difference
ΔG_{vol}	J/mol	Change in Gibbs energy from the formation of one unit volume of a second phase
J_B	$m^{-1}\,s^{-1}$	Flux of diffusion of substance B
L	m	Thickness of product layer
m	g	Mass
M	g/mol	Molecular weight
r	m	Radius
R_A	-	Reaction rate per unit area
$R_{V'}$	-	Reaction rate per unit bed volume
ρ	kg/m^3	Density
s	m	Distance within the reaction product layer
σ	J/m^2	Interfacial energy per unit area
T	°C	Temperature
V	m^3	Volume

V_0	m^3	Original volume
V'	m^3	Unit bed volume
X	-	Fraction number

Reaction rates

Symbol	**Units**	**Description**
a	-	Gas in adsorbed state
A	-	Pre-exponential factor, indicates rate of molecules in position to react per time
α	-	Mass change
E	J/mol	Activation energy
k	-	Rate constant
r	-	Reaction rate
R	J/K $\times$ mol	Gas constant
W	kg	Mass of sample
W_0	kg	Initial mass of sample
W_f	kg	Mass of sample after reaction

Temperature distribution calculations

Symbol	**Units**	**Description**
A	m^2	Cross-sectional area
α	m^2/s	Thermal diffusivity
c_p	J/kg $\times$ K	Specific heat
k	W/m $\times$ K	Thermal conductivity
m	kg	mass
r	m	Radius
ρ	kg/m^3	Density
t	s	Time
T	K	Temperature
T_i	K	Initial temperature
T_{max}	K	Maximum temperature the substance will be heated to
Q	J	Heat
q_x	J	Heat transfer rate in the x direction
$\dot{q}$	J	Heat transfer rate

Quartz

Symbol	Units	Description
A_f	-	Fraction of quartz remaining uncoverted after time t
r_0	m	Initial average radius
ρ	kg/m^3	Density
T	°C	Temperature
t	s	Time
u	m/s	Radial velocity of decomposition

X-ray diffraction

Symbol	Units	Description
$\mathrm{Corr}(W_\alpha)$	-	Corrected weight percent
n	-	Number of phases in analysis
S_α	-	Rietfeld scale factor for phase α
STD_{known}	mol/m^3	Weighted concentration of the standard
$STD_{measured}$	mol/m^3	Analyzed concentration
V	m^3	Volume of unit cell
$W_{amorphous}$	-	Weight fraction of amorphous phase
W_α	-	Weight fraction of the crystalline phases present in sample
ZM	kg	Mass of unit cell contents

Contents

Chapter 1

Introduction

1.1 Background

Silicon (Si) and ferrosilicon (FeSi) production is a carbothermic reduction where Si is produced in a submerged arc furnace (SAF). In Si production the main reactants are SiO_2 in form of quartz, and carbon (C) as reduction material in form of the raw materials coke, coal, charcoal and wood chips. Quartz, which is the low temperature, atmospheric pressure polymorph of silica (SiO_2), is the most important source of silicon for the silicon production. Since quartz is the second most abundant mineral in the earth's crust, it is an easily accessible mineral [1]. There are although several different types of quartz, and they all have different properties. During heating, quartz transforms into other phases. The acknowledged phase diagram, seen in figure 1.1, shows transformation into tridymite at 870°C and cristobalite at 1470°C. These phase transformations are heavily debated, and the phase diagram is said to be somewhat incorrect.

Silicon was originally used as an alloying element in the steel industry, and is still important for this purpose. It has in the recent years been an increase in the demand of silicon as it is discovered to be useful in a wider range of applications. The enhanced focus on renewable energy and the need of new ways of creating energy, gave a boost of production of energy through solar cells. This gave the need for more and better a solar cells with higher efficiency. To produce better solar cells, a demand of a more optimalized silicon production was created. In addition, a rise of silicon producers in low-cost countries is seen. Silicon producers in Norway and

other industrial, more expensive countries must now have a cost effective production to be able to compete with these countries [2].

With quartz as the most important raw material for silicon production, a deeper understanding of the behavior of silica is needed. The polymorphism of silica is one of the most studied systems, but also one of the least understood.

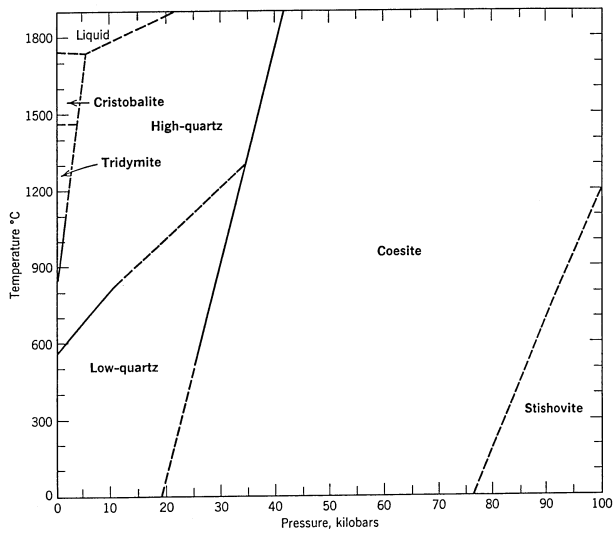

Figure 1.1: The phase diagram of SiO_2 as a function of temperature and pressure [3].

1.2 Aim of work

The goal for this master's thesis has been to get a better understanding of the phase transformations of quartz at high temperatures. This investigation is done by studying the mechanism and kinetics of quartz during heating. It is thought that the transition into cristobalite goes through an additional transition phase. This noncrystalline phase will also be investigated. The transformation to tridymite will not be investigated, since this is in later studies not considered a stable phase in pure quartz.

The goal for the thesis is to describe the mechanism and rate limiting parameters for phase transformations from β-quartz to β-cristobalite at conditions relevant for Si production. This is done by:

- Simulating the heating of quartz and find a temperature profile for different conditions.
- Experimental investigation of the amount of amorphous phase and cristobalite for different conditions.
- Investigating quartz visually during heating in wettability furnace and in light microscope after heating.

Different samples of quartz has been investigated after heat treatment and changing several parameters, to obtain a correlation when comparing all these samples. The analyzing method used to investigate the samples after heating is X-ray diffraction. In addition, samples will visually be investigated.

Chapter 2

Theory

2.1 Industrial production of silicon

To produce silicon (Si) industrially, a metallurgical process is conducted by reducing quartz (SiO_2) with carbon material, such as coke, coal, charcoal and wood chips. This reduction process is done in a submerged arc furnace. There is a general understanding that silicon carbide (SiC) and silicon monoxide gas are necessary intermediate products formed in the furnace. The total reaction, which is generally accepted for the silicon process, is expressed in equation 2.1.

$$SiO_2 + 2C = Si + 2CO \tag{2.1}$$

The different reactions occurring in the silicon furnace has previously been described by Schei et al. [4].

Raw materials is added at the top of the furnace where the temperature is around $1000-1300°C$. In the upper part of the furnace, descending material meets ascending SiO and CO gases and reaction 2.2, 2.3 and 2.4 occur. In the lower part of the furnace silicon is produced by reaction 2.5. In addition is SiO produced from SiO_2 by reaction 2.6 and 2.7 in the lower part of the furnace [5].

$$2C(s) + SiO(g) = SiC(s) + CO(g) \tag{2.2}$$

$$2SiO(g) = SiO_2(s) + Si(s) \tag{2.3}$$

$$3SiO(g) + CO(g) = 2SiO_2(s) + SiC(s) \tag{2.4}$$

$$SiC(s) + SiO(g) = 2Si(l) + CO(g) \tag{2.5}$$

$$SiO_2(s,l) + Si(l) = 2SiO(g) \tag{2.6}$$

$$2SiO_2(s,l) + SiC(s) = 3SiO(g) + CO(g) \tag{2.7}$$

These are the most essential reactions that occur in a silicon furnace and are needed to understand the processes of the silicon furnace. It should be noticed that reaction 2.6 and 2.7 are the same reactions as reaction 2.3 and 2.4 reversed.

Thermodynamically, the production of silicon requires a temperature above 1811°C and a silicon monoxide pressure high enough to drive reaction 2.5 to the right [2].

The modern type of silicon furnace is added a predefined mixture of raw materials consisting of quartz and reduction material, in addition to iron ore for ferrosilicon production. The charging of raw materials is done in cycles where the top of the charge is added and stoked down in the furnace towards the electrodes.

Aasly [6] described that since the raw materials are charged in batches, some of the quartz will probably experience higher temperatures and a larger temperature difference than quartz in the center of the newly charged batch. To decrease the difference in the temperature gradient, a more continuous charging could be used to get smaller batches.

A temperature profile has been made by Aasly [6], which shows that the average retention time for quartz in the furnace is about 5.7 hours. The minimum retention time is, however, probably between one and two hours. See figure 2.1.

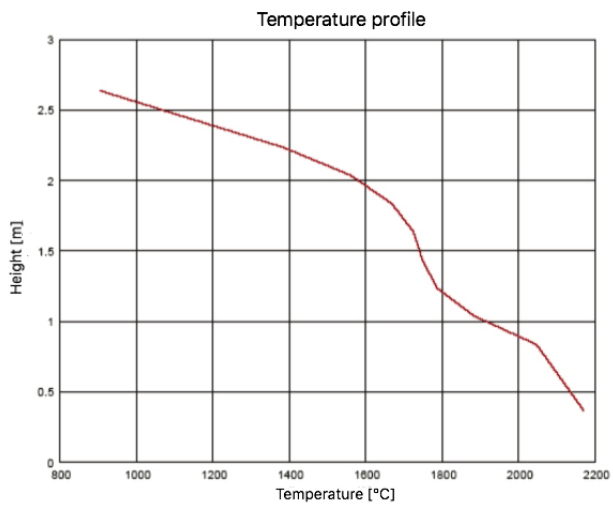

Figure 2.1: Calculated temperature profile of charged quartz in a silicon furnace. Explained by height in furnace as a function of temperature. Reprinted from [6].

2.2 Kinetics

2.2.1 Reaction between gas and solids

In dealing with reactions between gases and lumps of solids, it is of interest to relate the rate per unit mass or per unit volume of the reaction substance. This is explained by Rosenqvist [7].

The surface area per unit mass could be expressed by equation 2.8.

$$\frac{A}{m} = \frac{6}{d\rho} \tag{2.8}$$

In a bed of packed spheres, which is the case for the submerged arc furnace in the silicon production, the area per unit bed volume, V', is expressed by

$$\frac{A}{V'} = \frac{6(1-\epsilon)}{d} \tag{2.9}$$

Where ϵ is the void fraction. In close packing of spheres it is found that $\epsilon = 0.26$ for all sphere diameters. The reaction rate per unit bed volume could be expressed

as:

$$R_{V'} = -\frac{dn}{dt}\frac{6(1-\epsilon)}{A*d} \tag{2.10}$$

For non-spherical particles the same expressions may be used with the mean diameter:

$$d_m = \frac{6m}{A\rho} \tag{2.11}$$

Where A/m is the surface area per unit mass.

For the reaction between a lump of solid and a fluid phase, for example burning carbon in air, the reacting interface area is affected by the porous interface of the quartz.

Shrinking core model

The shrinking core model is further explained, also by Rosenqvist [7]. In the shrinking core model a reaction proceeds at the interface and move from the external surface of the lump towards its center. This forms a sharp boundary between the reacted and unreacted part in the interior of the lump. The limiting reaction rate is here affected of whether the reaction occurs on the interface or if there will be diffusion of the fluid or gas phase through the layer of reaction products. In the case where the interface reaction is the controlling reaction, the rate of reaction could for a spherical lump be expressed in terms of the original volume V_0, as seen in equation 2.12. This is the case when the reaction product is either very porous or if it is soluble in the fluid.

$$-\frac{dn}{dt} = \pi d^2 R_A = \frac{6d^2 R_A V_0}{d_0^3} \tag{2.12}$$

R_A is here the reaction rate per unit area. The initial and actual diameters are denoted d_0 and d, repectively. d^3/d_0^3 is can be expressed as $(1-X)$ where X is the fraction of solids which has reacted, then $n = V_0\rho(1-X)/M$, and

$$\frac{dX}{dt} = -\frac{dn}{dt}\cdot\frac{M}{V_0\rho} = \frac{6R_A M}{d_0\rho}(1-X)^{2/3} \tag{2.13}$$

M is the molecular weight.

When metal oxides react with reducing gases, there will be formed solid reaction products. These solid products will create a layer between the initial solid and the reacting gas. To precede the reaction by the shrinking core model, the material will have to be transported through this layer by diffusion. In most cases when the reaction increases the volume of the reaction product it creates a dense layer, and diffusion takes place through the crystal lattice. This would be the case if quartz transforms to cristobalite by the shrinking core model, unless cracks are created due to increased volume, since cristobalite theoretically has a 17 % larger volume than quartz [3].

The diffusion step might be the controlling, limiting step for some cases. The conditions at the reacting interface will here correspond to chemical equilibrium. When this is the case, the rate per unit area is proportional to the concentration gradient and the diffusivity of the diffusing substance in the product layer. The flux of the diffusion could be expressed by Fick's first law where the diffusing substance is denoted B.

$$J_{\mathrm{B}} = \frac{dn_{\mathrm{B}}}{dt} = D_B \frac{dC_{\mathrm{B}}}{ds} A \tag{2.14}$$

s denotes the distance within the reaction product layer, and A is the cross-section area. For reactions with lumps of solid substances, the relation between the diameter for the sphere, d_0, A, s and L, which is the thickness of the product layer, is shown in equation 2.15. The cross-section area is here $A = \pi(d_0 - 2s)^2$

$$\frac{dn_{\mathrm{B}}}{dt} = \frac{2\pi D_{\mathrm{B}} \Delta C_{\mathrm{B}}}{1/d - 1/d_0} \tag{2.15}$$

The different relations used in the calculations can be seen in figure 2.2

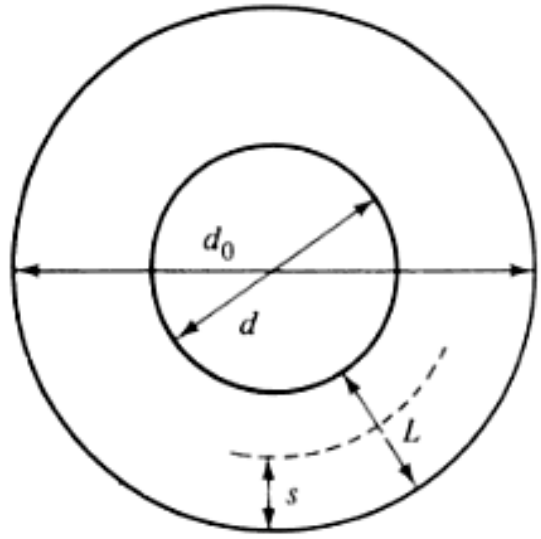

Figure 2.2: The shrinking core model for a sphere where d_0 = initial diameter, d = diameter of unreacted part, L = thickness of reacted layer, s = distance within layer. Reprinted from [7]

Nucleation

Heterogeneous reactions could also be characterized by formation of a new phase as explained by Rosenqvist [7]. Examples of these types of reactions are crystallization, condensation, and evolution of gases. In order for a new phase to grow, the interfacial energy between two phases must be overcome. In some cases this could affect the rate of the reaction. Thermodynamically, the Gibbs energy difference between the new and the old phase could be expressed by:

$$\Delta G = \frac{4}{3}\pi r^3 \Delta G_{vol} + 4\pi r^2 \sigma \tag{2.16}$$

ΔG_{vol} is the change in Gibbs energy associated with the formation of one unit volume of the second phase in macroscopic quantities, σ is the interfacial energy per unit area.

The formation of a new phase by nucleation could happen through heterogeneous nucleation, which is caused by a third phase. In this case the third phase is most possibly a solid impurity. If the interfacial energy between the third phase and the

product is less than the interfacial energy between the reactant and the product phase, nucleation of the product will be enhanced.

To what extent nucleation is the rate controlling reaction in metallurgical reactions has been a subject of discussion. The lack of nucleation may slow down the reaction [7].

2.3 Reaction rates

Reaction rates describe how fast a reaction reaches equilibrium. The knowledge of the kinetics of a reaction gives important information of both reaction rates under other environments than tested and the mechanism of the reaction. An introduction to this is given by Andersen [2].

The general definition of reaction rate is given in equation 2.18.

$$aA + bB = cC + dD \tag{2.17}$$

$$r = -\frac{1}{a}\frac{d[A]}{dt} = -\frac{1}{b}\frac{d[B]}{dt} = \frac{1}{c}\frac{d[C]}{dt} = \frac{1}{d}\frac{d[D]}{dt} \tag{2.18}$$

Where [A] is the amount of A.

If the reaction results in a mass change, the reaction rate could be measured by thermogravimetric analysis (TGA). This method measures the rate of mass loss of a sample at a given temperature. The results of the TG analysis is a curve showing how the mass has changed with respect to time. By differentiating this curve, the mass change is found. If gaseous products are the only products of the reaction, the reaction rate could be expressed as the rate of mass change as shown in equation 2.19.

$$r = \frac{dW}{dt} \tag{2.19}$$

If a solid product is formed, the mass change can be used to express the reaction rate by defining the parameter, α, shown in equation 2.20.

$$\alpha = \frac{W - W_0}{W_f - W_0} \tag{2.20}$$

Where W indicates the mass of the sample, W_0 is the starting mass of the sample, while W_f is the mass of the sample after completion of the reaction. The reaction rate could then be expressed as:

$$r = \frac{d\alpha}{dt} \tag{2.21}$$

The kinetics are dependent on several different parameters that affect the reaction rate. When modeling heterogeneous reactions, all these parameters are kept constant, which makes the reaction rate a function of these, and the temperature.

$$\frac{d\alpha}{dt} = f(\alpha) \cdot k(T) \tag{2.22}$$

The function $f(\alpha)$ is often said to describe the reaction mechanism or the physio-geometric kinetic model and should ideally be determined by how the reaction is controlled.

The temperature dependence is given by the rate constant k, and is described by Arrhenius relation, equation 2.23.

$$k(T) = A \exp\left(-\frac{E}{RT}\right) \tag{2.23}$$

E is the activation energy, R is the general gas constant, T is the temperature given in Kelvin and A is a pre-exponential factor. E, A and $f(\alpha)$ are often referred to as the kinetic triplet. In a homogeneous reaction, E is the energy barrier required for the molecules to react, while the pre-exponential factor, A, indicates the rate of molecules in position to react per time. The term $\exp(-\frac{E}{RT})$ could then be regarded as the probability of two colliding molecules reacting, while A is the number of colliding reacting molecules per second.

2.4 Temperature distribution calculations

2.4.1 Heat calculations

To calculate required heat to increase the temperature of a substance to a certain temperature, equation 2.24 could be used as described by Geankoplis [8].

$$Q = m \cdot c_p(T_{max} - T_i) \tag{2.24}$$

Where Q is heat required, m is mass of the substance, T_{max} is the temperature the substance will be heated to, and T_i is the initial temperature.

The transfer of heat by conduction follows Fourier's law as described by equation 2.25.

$$q_x = -kA\frac{\partial T}{\partial x} \tag{2.25}$$

Where q_x is the heat-transfer rate in the x direction in watts, A is the cross-sectional area normal to the direction of flow of heat in m^2, k is the thermal conductivity, $\partial T/\partial x$ is the derivative of T, which is given in K, with respect to x, with the other variables, y, z, and time t, being held constant.

2.4.2 Derivation of unsteady-state conduction equation

Unsteady-state conduction in one direction in a solid is described by Geankoplis [8] and could be explained by heat being conducted in the x direction in a cube with the size $\Delta x, \Delta y, \Delta z$. The conduction in the x direction is previously described by equation 2.25.

The heat balance for a cube can be written as:

$$Rate\ of\ heat\ input + rate\ of\ generation = rate\ of\ heat\ output + rate\ of\ accumulation \tag{2.26}$$

Where,

$$rate\ of\ heat\ input = q_{x|x} = -k(\Delta y \Delta z)\frac{\partial T}{\partial x}\bigg|_x \tag{2.27}$$

$$rate\ of\ heat\ output = q_{x|x+\Delta x} = -k(\Delta y \Delta z)\frac{\partial T}{\partial x}\bigg|_{x+\Delta x} \tag{2.28}$$

$$rate\ of\ heat\ accumulation = (\Delta x \Delta y \Delta z)\rho c_p \frac{\partial T}{\partial t} \tag{2.29}$$

ρ is density in kg/m^3 and c_p is the specific heat in J/kg·K

$$rate\ of\ heat\ generation = (\Delta x \Delta y \Delta z)\dot{q} \tag{2.30}$$

When eq. 2.27 - eq. 2.30 is substituted into eq. 2.26 and dividing by $\Delta x \Delta y \Delta z$ and letting Δx approach zero, equation 2.31 could be obtained.

$$\frac{\partial T}{\partial t} = \frac{k}{\rho c_p}\frac{\partial^2 T}{\partial x^2} + \frac{\dot{q}}{\rho c_p} = \alpha \frac{\partial^2 T}{\partial x^2} + \frac{\dot{q}}{\rho c_p} \tag{2.31}$$

where α is $k/\rho c_p$, thermal diffusivity. The derivation assumes constant k, ρ, and c_p.

For three dimensional purposes this derivation gives:

$$\frac{\partial T}{\partial t} = \alpha\left(\frac{\partial^2 T}{\partial x^2} + \frac{\partial^2 T}{\partial y^2} + \frac{\partial^2 T}{\partial z^2}\right) + \frac{\dot{q}}{\rho c_p} \tag{2.32}$$

In many cases, unsteady-state heat conduction is occurring but the rate of heat generation is zero. The unsteady-state heat conduction in three dimensions will then be

$$\frac{\partial T}{\partial t} = \alpha\left(\frac{\partial^2 T}{\partial x^2} + \frac{\partial^2 T}{\partial y^2} + \frac{\partial^2 T}{\partial z^2}\right) \tag{2.33}$$

For spherical particles, the equation above could conveniently for this case be expressed by

$$\frac{\partial T}{\partial t} = \alpha\left[\frac{1}{r^2}\frac{\partial}{\partial r}\left(r^2\frac{\partial T}{\partial r}\right) + \frac{1}{r^2 \sin\theta}\frac{\partial}{\partial \theta}\left(\sin\theta\frac{\partial T}{\partial \theta}\right) + \frac{1}{r^2 \sin^2\theta}\frac{\partial^2 T}{\partial \phi^2}\right] \tag{2.34}$$

Because it is assumed that the particles are spherical, it could be said

$$\frac{1}{r^2 \sin\theta} \frac{\partial}{\partial\theta}\left(\sin\theta \frac{\partial T}{\partial\theta}\right) = 0 \tag{2.35}$$

and

$$\frac{1}{r^2 \sin^2\theta} \frac{\partial^2 T}{\partial\phi^2} = 0 \tag{2.36}$$

so the equation becomes

$$\frac{1}{r^2} \frac{\partial}{\partial r}\left(r^2 \frac{\partial T}{\partial r}\right) = \frac{1}{\alpha} \frac{\partial T}{\partial t} \tag{2.37}$$

Where α is thermal diffusivity in m^2/s, r is radius of particle in m and T is the temperature in °C. This equation could be solved by explicit finite differences method.

2.4.3 Heating rate of quartz

The thermal diffusivity of quartz is according to Ksiazek et.al. [9] relatively high and it decreases up to the phase transformation from α-quartz to β-quartz, which occurs at 573 °C. From this temperature the investigated quartz shows a constant diffusivity value of 0.75 mm^2/s up to the phase transformation to cristobalite. The thermal diffusivity value of cristobalite is unknown. The thermal diffusivity of cristobalite is here assumed to be approximately the same as β-quartz. Based on this, the measured thermal diffusivity simulation of the temperature distribution to 300°C of a sphere has been performed. To do this, the equation for three dimensional unsteady-state heat conduction, equation 2.37, was used. The simulated temperature distribution is shown in figure 2.3. The temperature in the center of a particle of 4 cm is shown in figure 2.3a and a temperature profile in the particle after 500 sec in shown in 2.3b. The temperatures shown in these figures are different from the temperatures applicable for the silicon production, and just used as an example [9].

These figures show that the thermal diffusivity of quartz is high and the particle will be heated through rapidly when it is added to the submerged arc furnace.

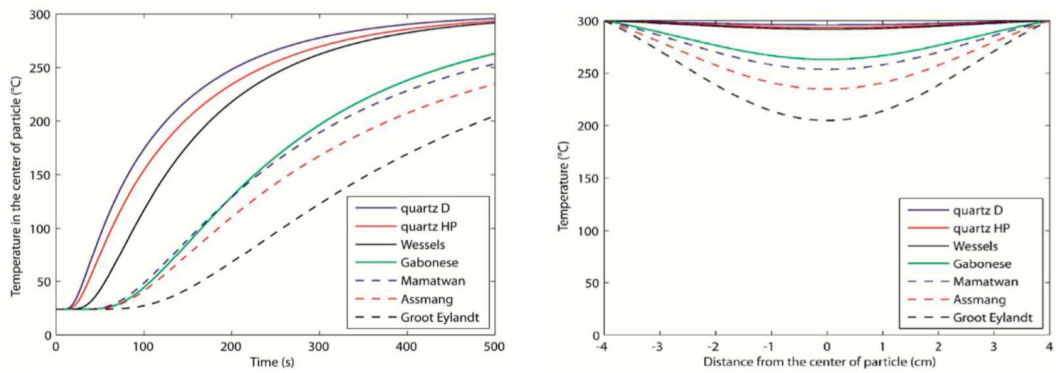

(a) Temperature in the center of a particle with radius = 4 cm heated to 300°C.

(b) Temperature profile in particles after 500 sec in 300°C.

Figure 2.3: Thermal diffusivity of different particles [9].

2.5 Quartz

Quartz is the second most abundant mineral in the earth's crust and is the low temperature, atmospheric pressure polymorph of silica, SiO_2. Resources of high purity quartz are found around the world. Pegmatite bodies and beach sand are the most frequent deposits utilized for this type of materials. Typical industrial use of high purity quartz is mainly for the electronic and semiconductor industry, and as optical fibers and crucibles [6].

The metallurgical quartz for silicon production needs to be 10 to 150 mm in size. This eliminates beach sand as a resource for this use [6].

2.5.1 Phases of silica

The SiO_4 tetrahedron is the basic building brick in all crystalline silica structures. This is a tetrahedron with Si in the center and O at all four corners and shows a mean Si-O-Si angle of 109°. The Si-O bonds have predominantly covalent character. The different ways of interconnecting these basic units by just one joint oxygen atom on one corner build the different structures of silica [10]. The basic unit and the crystal structure of α-quartz is shown in figure 2.4.

The different phases of silica stable at 1 atm as a function temperature is shown in figure 2.5. Additionally, the illustrated phase stability fields all have sub-fields

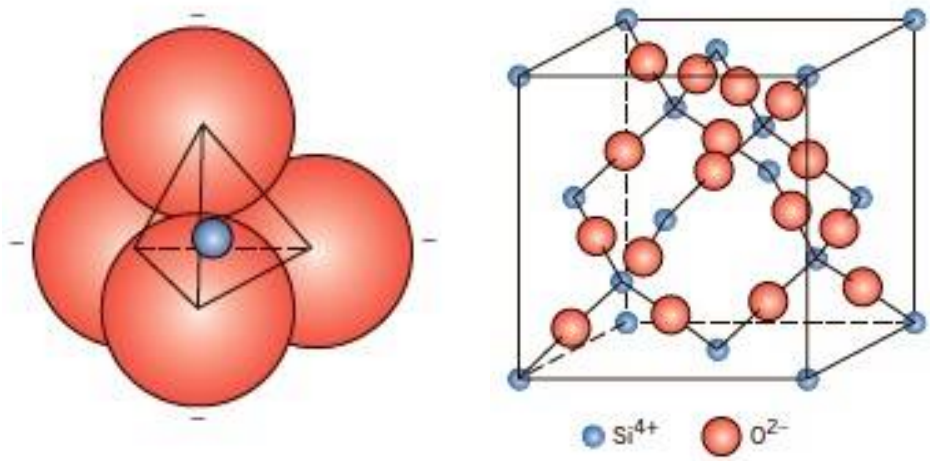

(a) Structure of quartz with a silicon atom in the center and four oxygens in tetrahedral positions around the silicon

(b) The Rhombohedral unit cell of α-quartz

Figure 2.4: Structure of quartz. Reprinted from [11].

with a low-temperature and a high-temperature phase. The low-temperature and high-temperature polymorphs in silica are called α- and β-polymorphs, respectively. α-quartz has a rhombohedral structure, β-quartz is hexagonal, while β-cristobalite has a cubic structure.

The stability of the crystalline phases based on standard free energy of formation with respect to temperature is shown in figure 2.6.

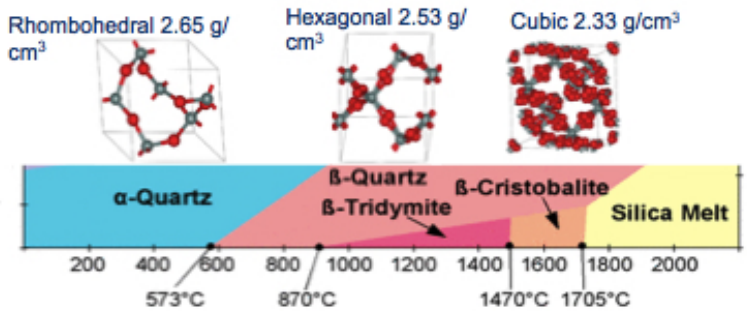

Figure 2.5: The phase diagram of SiO_2 around 1 atm and the crystal structures of the different phases at this pressure [5].

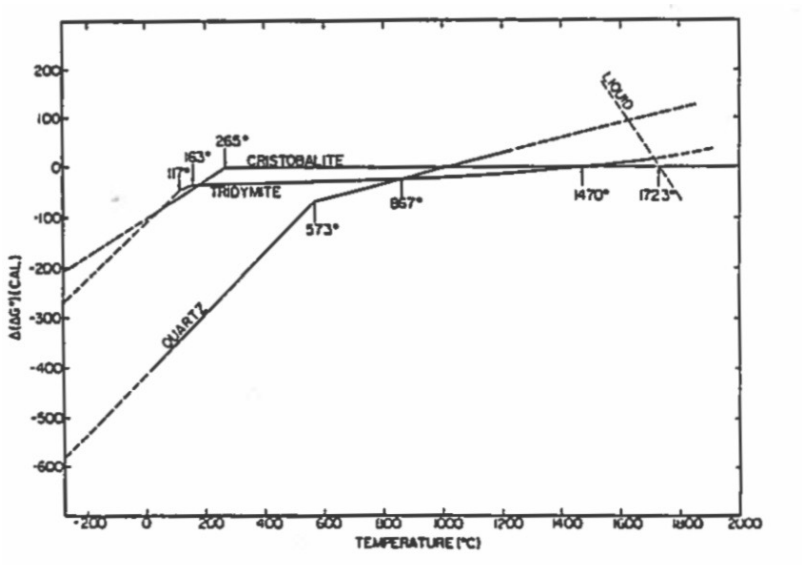

Figure 2.6: Standard free energy of formation for different phases of silica with β-cristobalite as reference state, as a function of temperature [12].

Several different melting temperatures of silica are reported in literature, but the most acknowledged is 1723°C [13]. It is although found softening and melting at lower temperatures. An example of this can be seen in figure 2.7 [14]. In a heating experiment to 1700°C with SiC in an induction furnace, it is found melted regions.

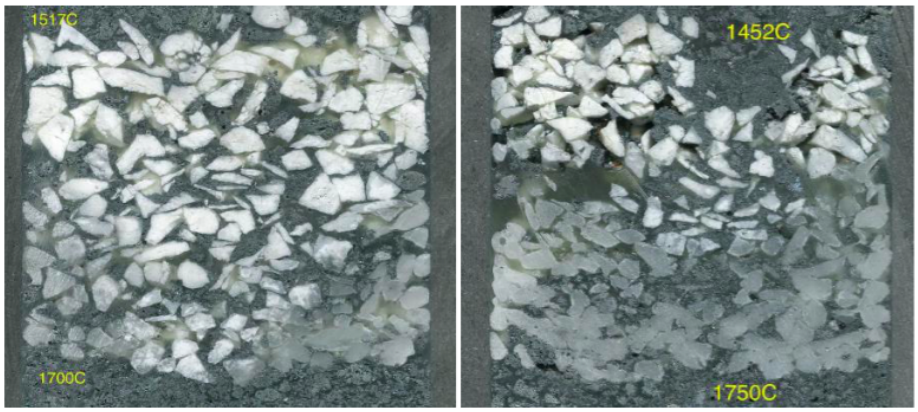

Figure 2.7: Quartz heated with SiC up to 1700°C in picture to the left and 1750°C to the right in an induction furnace. It could in the corners be seen melted and softened lumps of quartz [14].

2.5.2 The phase transformations in silica

The phase transformations in quartz during heating could possibly affect the yield and rate of the silicon production. Thus, the quartz-cristobalite ratio could be important for reactions involving SiO_2 in the production. Particularly is the rate of SiO formation from SiO_2, one of the main parameters affecting the temperature distribution in Si furnaces [1]. The most quoted and acknowledged study of high temperature phase transformations in quartz is also one of the earliest. This study was done by C. N. Fenner in 1913. This is also the study that the phase diagram of quartz is based on, as shown in Figure 2.5 and the relations is additionally presented in equation 2.38 [15].

$$Quartz \xrightarrow{870^oC} Tridymite \xrightarrow{1470^oC} Cristobalite \tag{2.38}$$

Stevens et al. [1] raised questions about the investigations done by Fenner because of the catalyst used in the experiments and the stability of the tridymite phase.

Silica goes through multiple polymorphic transformations at equilibrium. There are two different mechanisms of phase transformations. The Gibbs free energy might indicate that a spontaneous change should occur, but the kinetics of the structural changes varies depending on the mechanism of the phase transformation. For some

crystalline phases, only a minor change in the relative position is required for stabilizing the crystal structure. These small changes are called *displacive transformation* and occur relatively rapidly. For other crystalline phases, a transformation could include bond breakage and extensive rearrangement of atom positions. This is called a *reconstructive transformation* and are major structural changes that are relatively slow. Recontructive transformations includes atom movement and diffusional processes, by definition. A schematic illustation of the different tranformations can be seen in figure 2.8 [16].

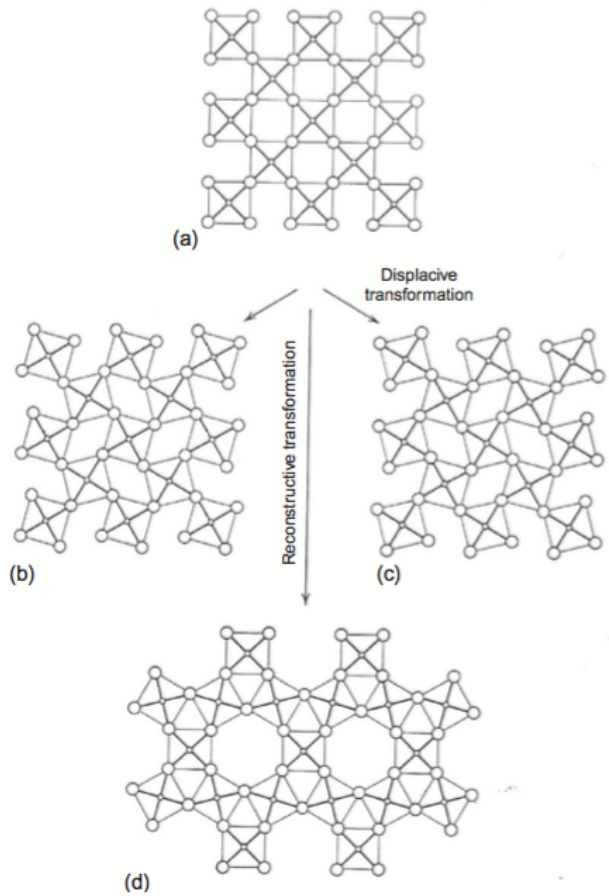

Figure 2.8: Schematic explanation for displacive and reconstructive transformation [16].

In silica, the phase transitions first established by Fenner as shown in equation 2.38, are reconstructive transformations. As already mentioned, these phases all have low-

and high-temperature polymorphs. An overview of all phases and transformations can be seen in figure 2.9.

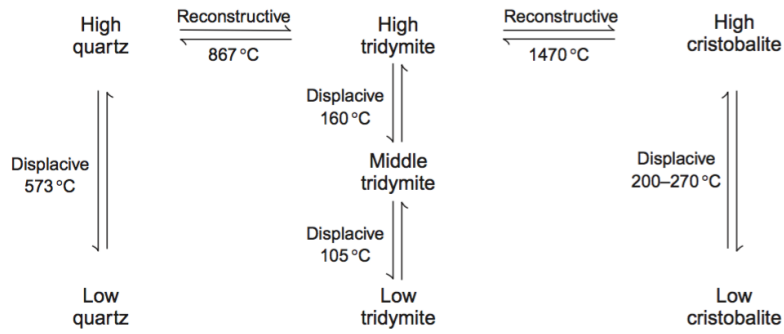

Figure 2.9: Illustration of transformations in silica at standard pressure [16].

The first step of the conversion from quartz to transition phase has been found to be a phase boundary process which follows equation 2.39 [17].

$$A_f = \left(1 - \frac{u \cdot t}{r_0}\right)^3 \tag{2.39}$$

Where A_f is a fraction of the quartz remaining unconverted after time t. u is radial velocity of decomposition, i.e. linear rate of propagation of quartz-transition phase boundary, and r_0 is the initial average radius of the particles present.

Wiik [17] claimed that cristobalite is assumed to be nucleated in the transition phase because this phase has a much lower density compared with quartz. The transition phase would therefore occupy a greater volume than the original phase and create tension in form of cracks. The further reconstructive transformation which involves breaking the Si-O bonds, results in an extensive fragmentation of the transition phase. It was in these studies found that large amounts of amorphous phase with no cristobalite looked opaque white and crumbled easily to powder. This could be an indication on a highly fragmented transition phase. It is therefore a possibility that a large number of homogeneously distributed internal nucleation centers would be available so that nucleation and growth of cristobalite would occur throughout the volume of the transition phase instead of being localized at the outer surface.

The volume expansion has previous been investigated by Salmang et al., and it was found that the volume expansion is more than 15 % at 1000°C and similar values

are valid for higher temperatures [18]. The temperature dependence of the specific volume of quartz, cristobalite and tridymite is shown in figure 2.10.

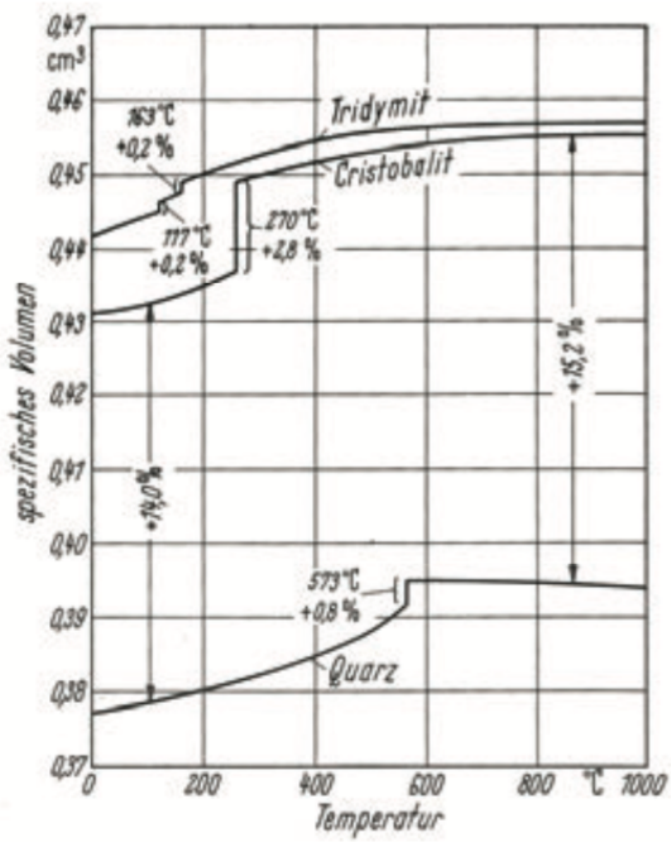

Figure 2.10: Specific volume as a function of temperature for quartz, cristobalite and tridymite. Reprinted from [18].

At room temperature and standard pressure conditions three crystalline silica phases, quartz, cristobalite and tridymite, can be found. This is because the conversion reaction from cristobalite/tridymite to α-quartz below $\sim$ 800°C is slow and weak. Figure 2.11 show a schematic plot of thermodynamically expected and observed phase transitions [10].

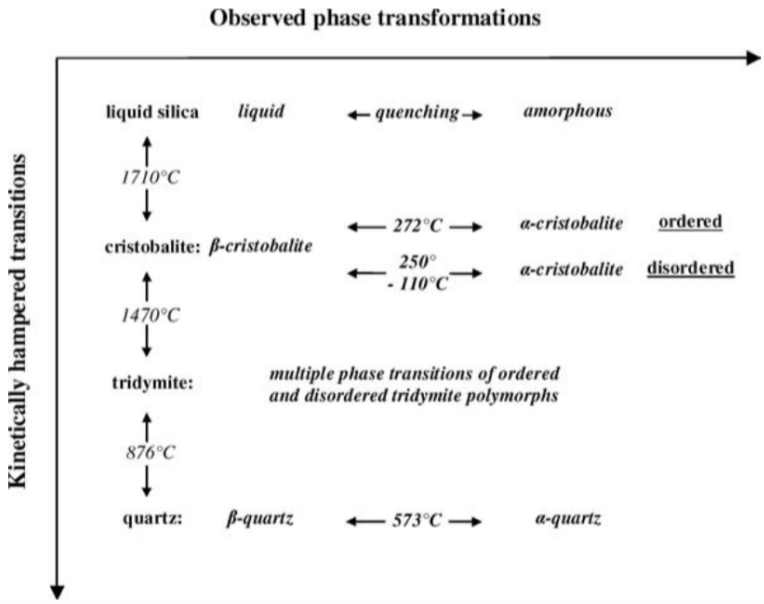

Figure 2.11: Illustration of relevant phase transitions within the unary system of SiO_2 with decreasing temperature [10].

The transformations from α-quartz to β-quartz and from β-quartz to HP-tridymite are ruled out as important for furnace operations and it will just be given a quick overview of these here. The importance of the transformation from β-quartz to β-cristobalite is yet not known, but it is known that the volume expansion in this transformation is large because of bond breakage [6].

The $\alpha - \beta$ transition in quartz

The $\alpha - \beta$-transition in quartz is as mentioned a displacive phase transition that occurs at $T_c = 573\,°\mathrm{C}$. Tucker et. al. [19] explained that in an extreme perspective it is assumed that the atoms hop between the positions corresponding to different α-domains. Thus, there will emerge dynamic disorder in the high-symmetry β-phase. During cooling the atoms progressively occupy the positions corresponding to one domain in the low-symmetry α-phase. It is thus a reversible transformation.

β-quartz to β-cristobalite

In a study done by Marians and Hobbs [20], it was found that to convert quartz into cristobalite about one third of the bonds must be broken and reformed. They also concluded that only one pair of crystal structure is stable against recrystallization and that any following bond breaking therefore will tend to drive quartz further from the crystalline state. Thus, it could be probable that the transformation of β-quartz to β-cristobalite goes via a disordered transition state, as seen in equation 2.40 [1]. In addition, Chaklader and Roberts [21] also established that the transformation from β-quartz to β-cristobalite involves an intermediate noncrystalline transition phase. It was in their study found that the transformation to the transition phase initially was slow. This is assumed to be due to a nucleation period. A more rapid conversion followed, presumably due to a propagation of the nucleated zones. The following reconstructive transformation into cristobalite is sluggish [17]. This will be further looked at later in the theory.

$$Quartz \xrightarrow{>\approx 1300^oC} Transition\ phase \rightarrow Cristobalite \tag{2.40}$$

It is from this expected to find an amorphous phase in quartz after heating.

Natural silica materials was investigated by Schneider et al. [22] in the temperature interval 1100 to 1600°C to study the transformation of β-quartz to β-cristobalite. The quartz decomposition in the natural samples initially proceeds rapidly but reaches saturation after about 60 minutes of firing. The study also supports the theory of β-quartz to β-cristobalite conversion processes with formation of an intermediate amorphous transition phase. The samples investigated here contain $SiO_2 \geq 95$ wt%. The main impurity oxide is CaO (1.5 to 3.5 wt%). Mitra [23] has previously suggested that the conversion of quartz to the transition phase is boundary-controlled, and that the conversion of the transition phase to cristobalite is concentration-controlled. This means that the transition to β-cristobalite involves an induction period where total absence of cristobalite is expected until enough amorphous phase is produced for the required concentration enabling the formation of cristobalite [6]. Poe and Kuelmer [24] assumed that the transformation from β-quartz to β-cristobalite proceeds under an intermediate formation of partially disordered cristobalite rather than a non-crystalline melt. The rate of the transition to β-cristobalite is considered significant for the thermo-mechanical properties of the quartz raw materials in the initial phase in the silicon furnace [18].

The transformation from β-quartz to β-cristobalite has previously been investigated

by Kjelstadli [15]. It was in this study found that the transformation to cristobalite is slow. Various quartz types were heated to 1600°C with three different hold times. The results can be seen in figure 2.12, where Qz 9 is a quartz type with confidential name. Qz 29 is a Faleq. It is additionally found large differences between the different quartz types.

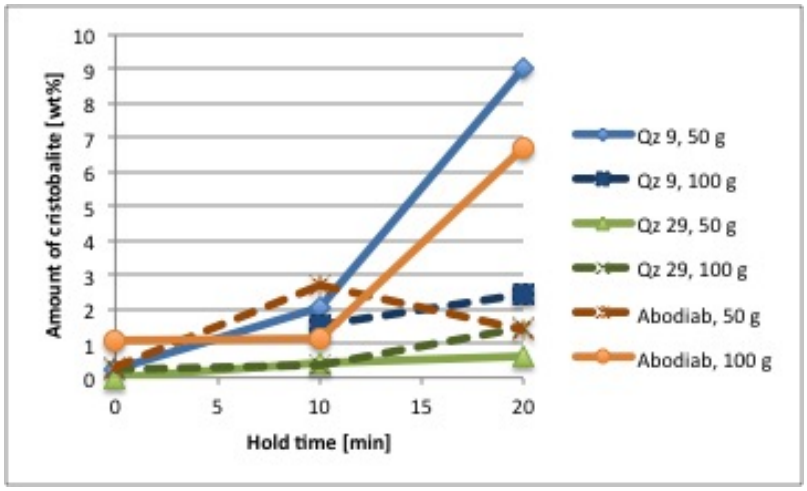

Figure 2.12: The amount of cristobalite as a function of hold time at temperature 1600°C in different quartz types [15].

The amount of amorphous phase was, however, found to be much higher than the amount of cristobalite for all quartz types, as seen in figure 2.13. This supported the theory that the rate limiting reaction is the reconstructive transition from transition phase to cristobalite.

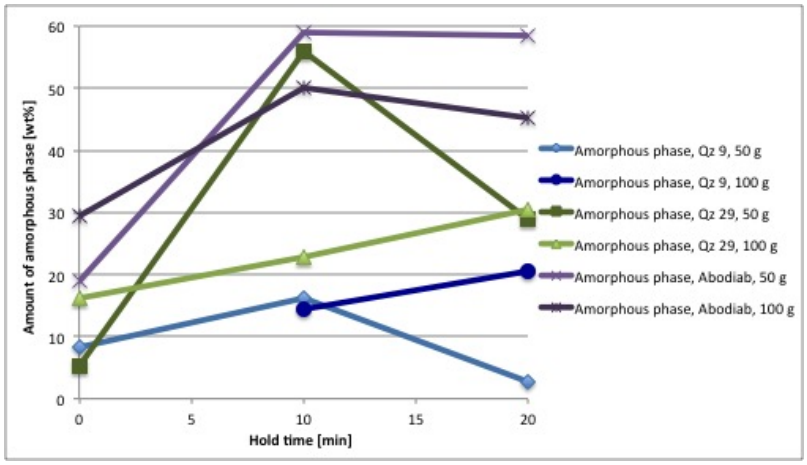

Figure 2.13: The amount of amorphous phase as a function of hold time at temperature 1600°C in different quartz types [15]

As mentioned earlier, quartz has high thermal diffusivity [25]. This might decrease any size effect of the quartz particles as the heating of particles not seem to be the rate limiting factor. In the previous study it was not found any clear size effect between particles of 50 g and 100 g.

Two different studies have been done on the same quartz type, Qz29 (Faleq), one with shorter hold time (0-20 min) [15] and one with longer hold time (15-60 min) [26]. It was then seen that the transition rate seemed was highest between 30 and 40 minutes, as shown in figure 2.14.

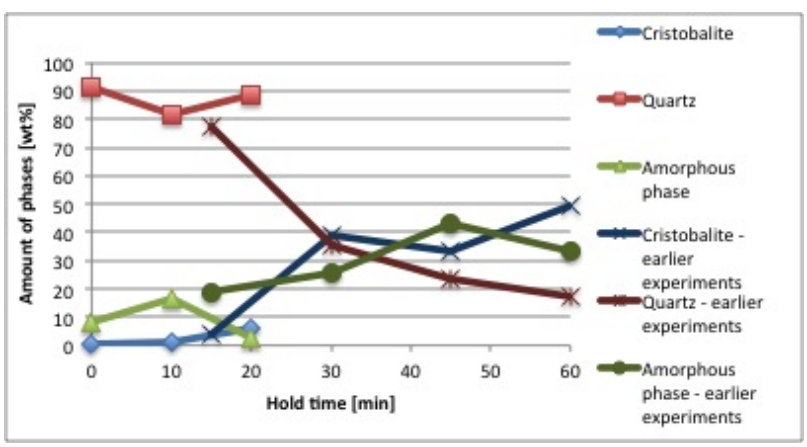

Figure 2.14: The amount of phases in samples of Qz 9 after heating to 1600°C [15].

The specific surface has been investigated by using BET analysis. The two sizes of particles were plotted against hold time. This could be used for calculating the volume expansion during heating, and could be compared for the amount converted from β-quartz. The results for Qz29 can be seen in figure 2.15.

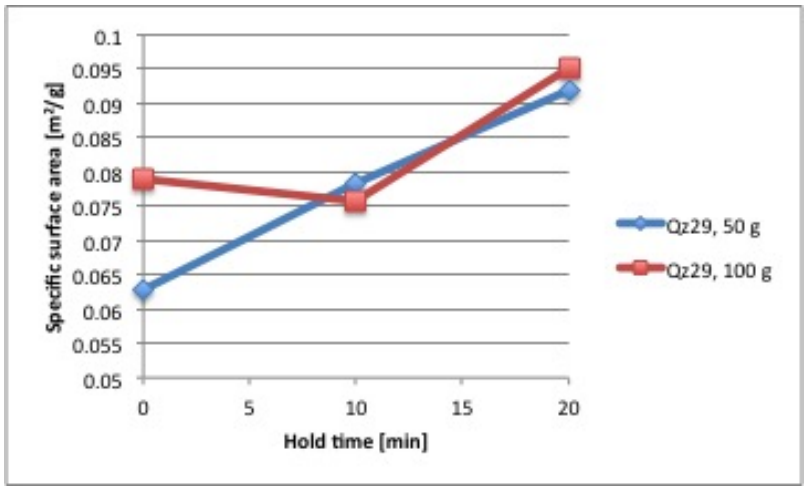

Figure 2.15: Specific surface area for Qz29 (Faleq) after heat treatment measured by BET plotted against hold time [15].

Crystallization of amorphous silica to β-cristobalite

Linear crystallization of β-cristobalite out of amorphous silica has been studied by various researchers under dry thermal conditions. Presser et al. [10] described that water increases the crystallization rate significantly, thus environmental conditions affect the crystallization to β-cristobalite. Formation of β-cristobalite has been found to take place after about 20 hours between 1100°C and 1200°C. Above 1400°C, the crystallization takes place at a much shorter time period, in the range of minutes. In addition to temperature and oxidation time, the presence of additives, impurities and surface morphology have an influence on crystallization speed. It could be assumed that the crystallization starts at structural imperfections and at the sample's edge [10].

The crystallization rate of amorphous silica toward β-cristobalite was by Presser [10] found to reach a maximum at 1677°C. At higher temperatures, the silica layer becomes more fluid and the β-cristobalite grain boundaries will not be able to further react.

The crystallization of amorphous silica will affect the diffusion of oxygen and reaction gas above 1150°C as more and more silica is transformed to β-cristobalite. The amorphous networks of silica consist of a statistic arrangement of small structural units. This model coincides with the crystallite theory, which explains that amorphous silica consists of microcrystalline forms of various crystal modifications or at least of parts of their unit cells. One of the most striking theories to why amorphous silica undergo a phase transformation to β-cristobalite is the interpretation of amorphous silica as a very distorted form of fractured structural units of β-cristobalite. This explains the small difference between the density of amorphous silica and β-cristobalite, where $\rho \approx 2000 - 2200\ \mathrm{kg \cdot m^{-3}}$ and $\rho = 2200\ \mathrm{kg \cdot m^{-3}}$, respectively [10].

The kinetics of crystallization can be divided into three steps. During the first step, nucleation and subsequent growth of future crytallization centers will occur. This is a process that especially depends on temperature and will be accelerated by impurities like water and sodium. The impurities can also prevent a complete crystallization by stabilizing small regions of amorphous silica. The Arrhenius equation, which is shown in 2.23, can be used to characterize the correlation between the nucleation rate and the temperature. When the nuclei reaches a critical size, the crystal growth will increase in the crystallization centers. Nucleation will require higher activation energies than crystal growth. In the last step an equilibrium phase will be established [10].

Tridymite-cristobalite relations

Cristobalite and tridymite are structurally related and polytypic. β-cristobalite shows only trans-connected pairs of tetrahedra, while β-tridymite shows both trans- and cis-configuration. Because of this, the stacking order related property is destabilizing the ideal β-tridymite structure. The β-tridymite structure consists of two kinds of layers (AB), while the β-cristobalite in contrast have a stacking sequence that is three-layered (ABC) [10].

The tridymite phase is, as already mentioned widely debated and most published phase diagrams include tridymite as a stable phase with 1470°C as the tridymite-critobalite transformation. It is although generally accepted that in many systems, cristobalite crystallizes from amorphous phase within the tridymite stability range. Flörke stated in 1955 that tridymite is not a stable phase, but is dependent on the presence of impurities [27]. Tuttle and England claimed that tridymite did not need

any other impurity than water to be stable [28]. Hill and Roy did however establish an existence of a stable tridymite phase [29]. Later, Roy and Roy [30] presented additional evidence of the existence of transformation between stable tridymite and stable cristobalite.

The cristobalite $\alpha - \beta$ inversion

The high temperature form of cristobalite, β-cristobalite, has oxygen atoms arranged in a cubic close-packed form. The low temperature structure, the α-structure, has a distorted form of the high temperature structure where the bond angles of Si-O-Si change. The high temperature cristobalite structure is a more idealized stacked form with three layers with the sequence: ABCABC... The low temperature form of cristobalite is said to have a stacking sequence like tridymite with only two layers: AC'AC'AC'..., where C' is stacked in the same way as C but with a rotation of 180 °, in addition to the three layered high temperature structure. This low temperature cristobalite phase is usually referred to as disordered cristobalite, C_{D} [31]. β-cristobalite is stable between 1470°C and the melting point at 1723°C [13]. When cristobalite reaches a temperature that is below $\sim$ 270°C, it goes through a reversible first order phase transition from β-cristobalite which is space group $\mathrm{Fd\bar{3}m}$ to α-cristobalite which has space group $\mathrm{P4_12_12}$. This phase transition results in a volume decrease of 6.2 vol% and gives crack formation in a silica rock during cooling [10].

Pagliari et al. [32] described that α- and β-cristobalite have average bulk thermal expansion values of 91.7 and $6 \times 10^{-6}\,°\mathrm{C}^{-1}$, respectively. This remarkable different thermal dilation affects the shrinkage upon cooling of the traditional ceramic bodies.

2.5.3 Size effects on silica polymorphism

The sintering behavior of approximately monosized SiO_2 has previously been studied by S. Wu et al. [33] and it was then found that highly ordered structures start densifying without crystallization at 1000 °C. There is, however, a requirement of an initially orderly packed body. From SEM examinations with four different particle sizes, it was found that samples with larger particles show a much broader size distribution. After sintering at 800, 900 and 1000 °C, it was found that the samples with the two smallest particle sizes (7-10 and 10-13 nm) transformed to tridymite at

900 and 1000 °C, but were amorphous at 800 °C. The samples with larger particle sizes (50 and 80 nm) remained amorphous at the three different temperatures.

Pagliari et al. [32] found that the stage of advancement of any high temperature transformation depends on the particle-size-distribution (PSD) of the involved materials and firing-time experienced. The kinetics of the phase transformation from quartz to cristobalite is an important step to understanding the kinetics and energetics of the whole high temperature process. Experiments showed that the smaller average particle size, $\langle \mathrm{d} \rangle$, the smaller volume-average domain size, $\langle D_v \rangle$ is found. A decrease of the particle size is accompanied by an increase of the peak's broadening. This indicates a general reduction of the crystalline domain size and increase of root mean square (RMS) strain, which means that the transition drives the sample further from crystalline state. After doing experiments at 1200 and 1300 °C it was found that rising the temperature with 100 °C causes the amount of formed cristobalite to increase by more than 6 times for the smallest particle size and by 2-3 times for the coarsest one. The difference of the crystalline domain size of quartz, ΔD_v, has also been studied, and it was found that the coarsest samples show a negative value for ΔD_v. This exhibits a larger average crystallite size after heating because of grain growth. However, it has been found that the samples with a small $\langle \mathrm{d} \rangle$ have smaller average crystallite size after heating, which could indicate that the reactions occurring during cooling might have an influence on the correlation of the domains that tend to break due to the volume difference of the involved polymorphs. Neither ΔD_v and ΔRMS strain do not show any dependence on how the sample is prepared. From this it seems as the particle dimensions played an important part in the cristobalite formation.

2.6 X-ray diffraction

To identify which phases are present and to quantify these phases, the samples could be analyzed with quantifying X-ray diffraction. XRD is an analyzing technique that uses electromagnetic radiation by accelerating electrons towards a metal target. The analysis is easy when the sample is crystalline. It will then emit monochromatic radiation peaks from the sample. The X-rays have a known wavelength when they hit the sample. It will then reflect the rays according to Bragg's law which gives an unique reflection pattern for each crystalline structure. The quantification is done by comparing the reflecting intensity peaks of the different phases [34]. More often than not, the sample contains an amorphous phase. Crystalline materials are defined as

solids with fixed volume, fixed shape and a long-range order, which is bringing about structural anisotropy and will therefore produce sharp diffraction peaks in a XRD analysis [35]. Amorphous phase is defined as substances that show no crystalline nature whatsoever by any of the means available for detecting it [36]. Amorphous materials are thus solids with fixed volume, fixed shape that is characterized by short-range order, which also could have loose long-range order [35]. The quantization of amorphous phase is therefore complicated and the accuracy is debated.

2.6.1 Internal standard method

The most common approach of quantitative phase analysis of an amorphous material with XRD is what is called the internal standard method, described by Madsen et al. [35]. For the internal standard method, the weight fraction W_α of the crystalline phases present in each sample is first estimated using the algorithm of Hill and Howard:

$$W_\alpha = \frac{S_\alpha (ZMV)_\alpha}{\sum_{j=1}^{n} S_j (ZMV)_j} \tag{2.41}$$

Where S_α = the Rietveld scale factor for phase α,
ZM = the mass of the unit cell contents,
V = the volume of the unit cell,
n = the number of phases in the analysis.

This method is the most common for the quantitative phase analysis (QPA) and it relies on the assumption that all phases in the sample are crystalline and have been included in the analysis. Therefore, equation 2.41 sums the analyzed concentrations to unity.

The sample is in this method spiked with a known, accurately mass of a standard material that is extremely crystalline. The weight fractions of the crystalline phases present are calculated with equation 2.41. The presence of a known weight fraction of a crystalline internal standard material in the sample could then calculate a corrected weight fraction based on the already calculated weight fraction in the crystalline phases, as shown in equation 2.42.

$$\mathrm{Corr}(W_\alpha) = W_\alpha \frac{STD_{known}}{STD_{measured}} \tag{2.42}$$

Where	Corr (W_α)	=	the corrected weight percent,
	STD_{known}	=	the weighted concentration of the standard in the sample,
	$STD_{measured}$	=	the analyzed concentration derived from Eq. 3.23

When the corrected concentrations is calculated, the weight fraction of the amorphous material could be found from equation 2.43 [35].

$$W_{amorphous} = 1 - \sum_{j=1}^{n} \mathrm{Corr}(W_j) \tag{2.43}$$

2.6.2 Accuracy of analysis method

To assess the individual performance of each method, the bias in the amorphous content has been calculated from equation 2.44:

$$\mathrm{Bias} = \mathrm{Analyzed} - \mathrm{Weighed} \tag{2.44}$$

Most of the analyzes fall within ± 2 wt% of the weighed amount. This is an absolute measure and does not take into account the level at which the amorphous content is present [35].

Chapter 3

Experimental

3.1 Quartz samples

3.1.1 Samples for experiments in air

To study the conversion rate from quartz to cristobalite in air, one type of quartz were heat treated to 1600 °C and 1700°C with five different hold times and four different sizes of quartz particles in total 21 different experiments as shown in table 3.1.

The quartz type used in these experiments is called Qz29 which is a Faleq and is provided by Reliance. As seen in table 3.1 some samples were done in multiple parallels. Because of results that seemed unreliable compared to the other results found from analysis, some samples were run in several parallels. Sample 3 was additionally run to investigate the accuracy of the experiments and the liability of the results. Sample 4, 11 and 19 was also analyzed twice with XRD. This was done to see the deviation of the XRD analysis.

The heat treatments were done to study the rate of the transformation from quartz to cristobalite and the transition state with the amorphous phase and when this phase is most prominent. In addition, the kinetics and mechanism for heat distribution in particles of different size and different types of quartz have been studied.

Table 3.1: Overview over the heat treatments done on the different samples of quartz in air.

Sample	Temp. [°C]	Hold Time [min]	Weight of Particle [g]	No. of Parallels	No. of XRD analysis
1	1600	30	50	1	1
2	1600	40	50	1	1
3	1600	30	100	3	3
4	1600	40	100	2	3
5	1700	0	50	1	1
6	1700	10	50	1	1
7	1700	20	50	1	1
8	1700	30	50	1	1
9	1700	40	50	2	2
10	1700	0	100	1	1
11	1700	10	100	2	3
12	1700	20	100	1	1
13	1700	30	100	1	1
14	1700	40	100	1	1
15	1600	0	10	1	1
16	1600	20	10	1	1
17	1600	40	10	1	1
18	1600	0	200	1	1
19	1600	20	200	2	4
20	1600	40	200	1	1
21	1600	10	50	1	1

3.1.2 Sample preparation

A hammer was used to shape out particles with the right size. It was difficult to shape out samples of exact weight, so a particle of the desired weight ±10 % was accepted. This was thought to be acceptable since the configuration of the particles give a variation in radius, even though the weight would be the same for the samples. After heating, the same hammer was used to shatter the particle into small grains so that it would be suitable for further analysis and so that it would be possible to split out a randomized sample. To get a randomized sample, the shattered particle was separated out with a splitter until a desired amount of quartz, which is about 2 grams, was obtained for XRD analysis.

Some samples were too hard to crush with a simple hammer, so a crushing machine with boron carbide was used to crush the sample for preparation to XRD analysis.

For experiments attempted done in CO gas, grains of 1-3 mm were used in a sample of total 2 grams. These were also crushed to the desired size by a crushing machine, and the rest were separated out by sieving.

3.1.3 Samples from furnace excavation

During a furnace excavation, three samples of quartz were obtained. The furnace is at Wacker's plant at Holla. The quartz type used in the furnace is from Tana, Faleq and Erimsa. The samples were taken from the top charge in the furnace in different distances from the electrodes, see figure 3.1, with sample 1 furthest from the electrodes and sample 3 closest. The temperature in the area is expected to have been between $800 - 1300°C$. The time of exposure is unknown.

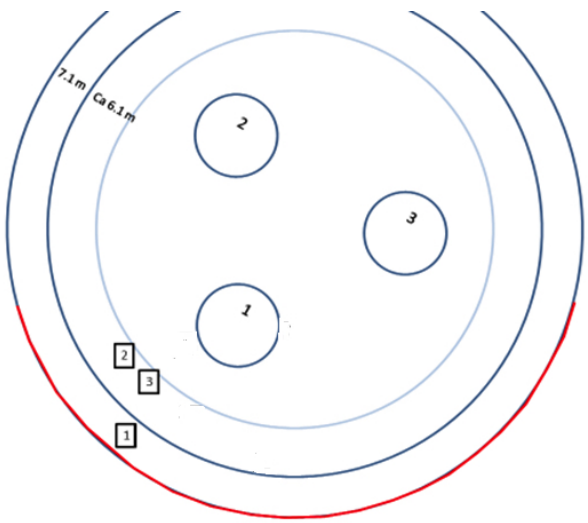

Figure 3.1: Sketch of the positions of the investigated excavated quartz samples

The samples from the furnace were crushed so that one sample from the edge and one sample from the center of the particle could be obtained. This was done to find any possible size effects. In total six samples could then be analyzed in XRD, as will be explained later in this chapter.

3.2 Heating of quartz

The heat treatment was done in a rapid heating furnace. Because of unfortunate incidents with the furnace originally used, two different furnaces had to be used. The original heating program was attempted to be imitated as far as possible. The original furnace, a Nabertherm LHT04, and where the thermocouple in the middle of the furnace was placed is shown in figure 3.2a. The dimensions of the furnace is sketched on the figure. The sample was placed just beneath the thermocouple. The thermocouple that measures the temperature in the middle of the furnace is placed in the white tube in the center. This thermocouple will then measure the temperature where there is a lot of heat radiation. Since the thermocouple is placed inside an alsint tube, it will although not obtain the same direct heat radiation as the particles does. There is also a thermocouple installed in the furnace wall to measure the temperature in the environment where the heat radiation is not as present. The two measured temperatures are similar, as can be seen from figure 3.3. The temperature measured by the thermocouple in the middle of the furnace changes more rapidly, while the temperature in the furnace wall changes more continuously. Both of the thermocouples are B-type thermocouples, which are logged with an Omega HH1384 thermologger.

As a furnace substitute for the previously described furnace, an Entech rapid heating furnace was used. The inside of this furnace can be seen in figure 3.2b. This furnace was used for both rapid heating of quartz particles in air and heating of quartz samples in CO atmosphere. As can be seen from the figure, the dimension of this furnace are similar to the original furnace.

The logged temperatures for all the samples heated in the Nabertherm rapid heating furance is shown in figure 3.3. It is seen that the heating curves are similar for all samples.

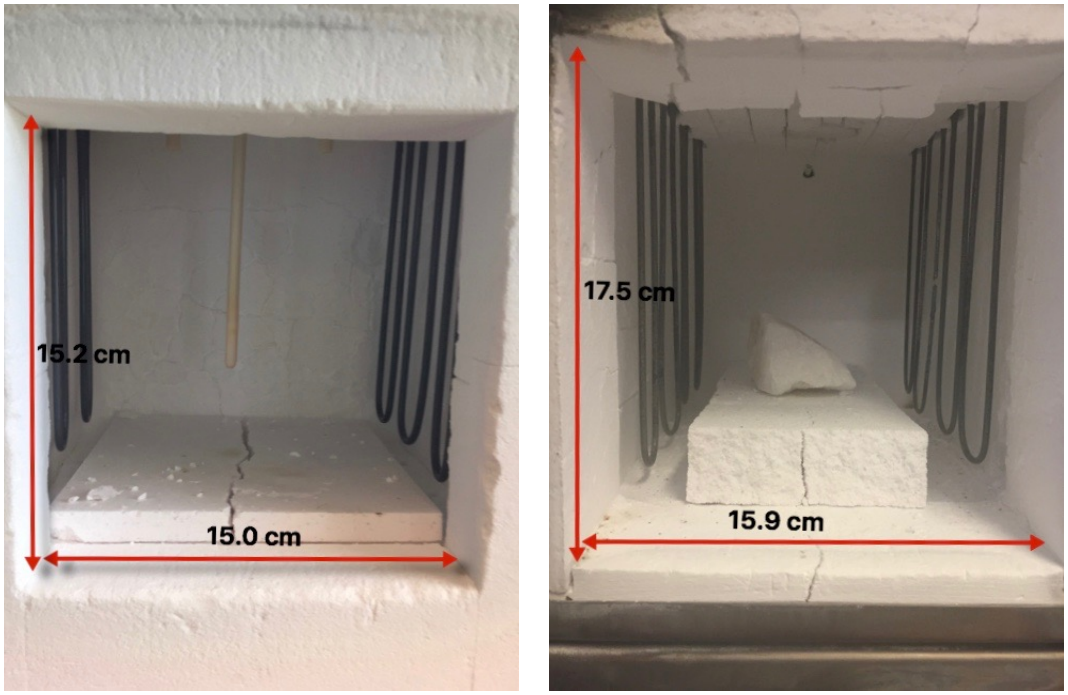

(a) Ovn 1, Nabertherm (b) Ovn 2, Entech

Figure 3.2: The interior of two different rapid heating furnaces used for heat treatment of quartz.

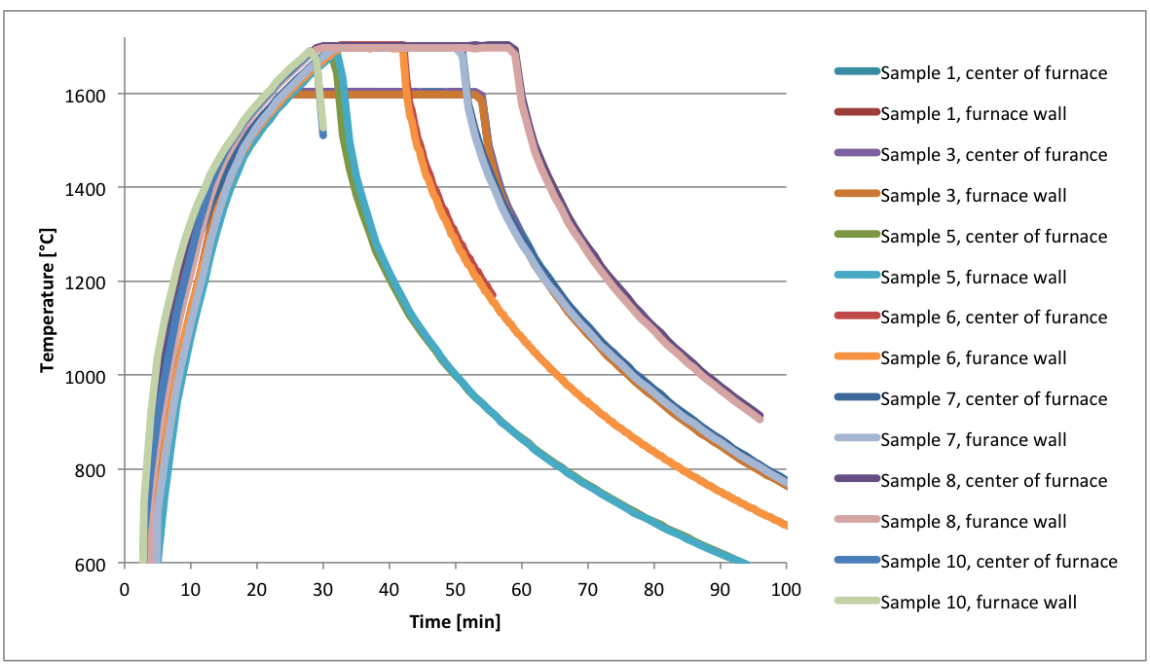

Figure 3.3: Temperature profiles for the samples heated in Nabertherm furnace.

The temperatures for the Entech furnace were logged for heating to 1600°C and 1700°C for 30 minutes. These temperatures were not logged during the experiments, but measured after they were finished. The logged temperatures can be seen in figure 3.4.

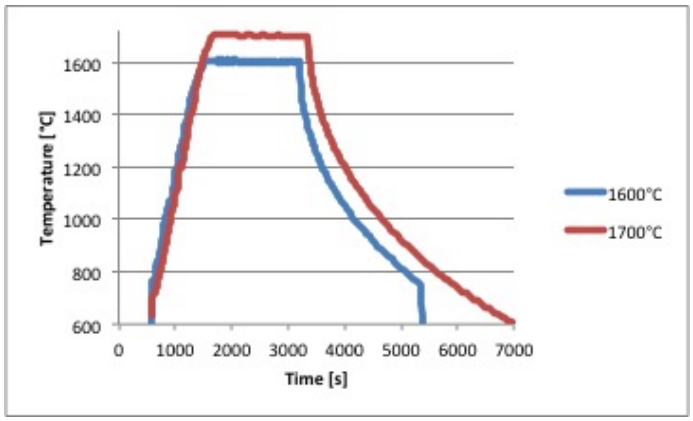

Figure 3.4: Temperature profiles for heating to 1600°C and 1700°C in Entech furance with 30 minutes hold time.

A temperature profile was measured by using the thermocouple and the thermologger and moving it upwards in vertical direction. The profile can be seen in figure 3.5. It could from this be seen that the temperature is lower higher up in the furnace. The temperature difference found was about 30°C from top to bottom, but the difference in the region where the sample is placed is about 5°C.

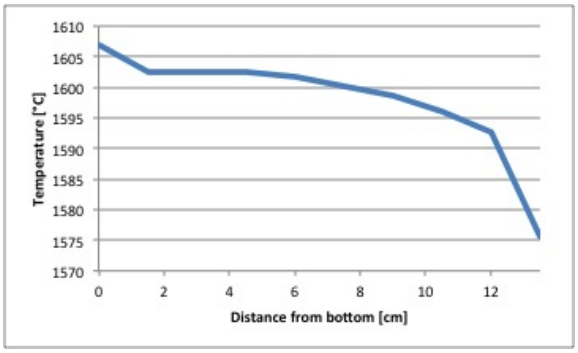

Figure 3.5: Temperature profile of the furnace used showing temperature as a function of distance from the bottom of the furnace

3.3 Modeling the heating of quartz

To understand what the rate limiting factor is during heating of quartz, the time needed to heat quartz to target temperature was calculated. This was done by calculating the heat transfer in quartz. A quick estimate by calculating the heat convection of quartz by equation 2.24 was first found. This was compared to the amount of heat needed to heat up the particle to the desired temperature, calculated by equation 2.25. From this, an estimated time of heating could be obtained. This estimate could be seen in table 3.2. It was here assumed that the particle is a perfect sphere. The radius was calculated based on the density of quartz, which is as an average found to be 2.62 kg/m^3 [37], and the weight of the particle.

Table 3.2: Heat transfer in quartz and amount of time until completely heated through.

Mass [g]	**Heat [J]**	**Heat transfer rate [J/s]**	**Time before heated through [min]**
10	18900	383.76	0.82
50	94500	656.22	2.40
100	189000	826.78	3.81
200	378000	1041.7	6.05

To further investigate the heat transfer of quartz, a simulation for a single particle was performed. This simulation is based on the unsteady-state equation, eq. 2.37, and can be seen in figure 3.6. The simulation was done in cooperation with M. Ksiazek. The radius of the particles are varied, and the simulation is done for two temperatures, 1600° and 1700°C. The thermal diffusivity value used is 0.75 mm^2/s and is assumed constant above 573°C. The simulation takes into account that the furnace uses 24 minutes to heat to 1600°C and 30 minutes to heat to 1700°C.

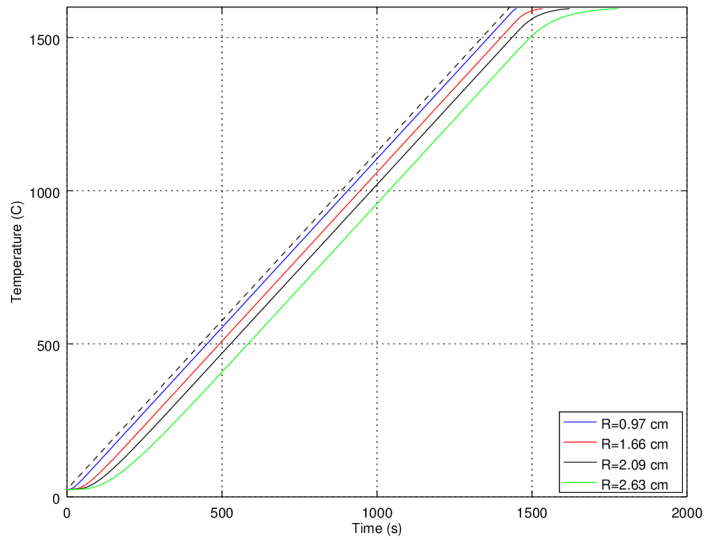

(a) 1600°C

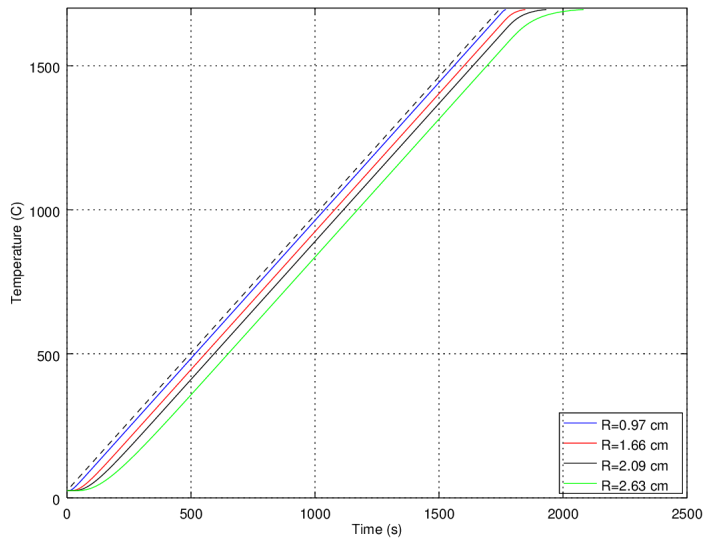

(b) 1700°C

Figure 3.6: Simulation of heating of quartz particles of different sizes, done in co-operation with M. Ksiazek. Heating to 1600°C takes approximately 24 min and to 1700°C it takes about 30 minutes.

3.4 Setup for experiments in CO atmosphere

For experiments in CO atmosphere, a more complex experimental setup was used as shown in figure 3.7. The procedure for heating in CO was to first heat the furnace to 1500°C with a heating rate of 500°C per hour. The heating rate had to be limited because the alsint tube could be damaged. It was attempted to mount the sample as shown in figure 3.7. Here, a thermocouple and a gas outlet was placed right above the crucible. A sample of about 2 grams of 1-3 mm quartz grains was placed in the crucible. The crucible was attached to the thermocouple by hanging it in a platinum wire. This was all placed in an alsint tube. All the different tubes were hanged in a plug that closes the atmosphere in the tube.

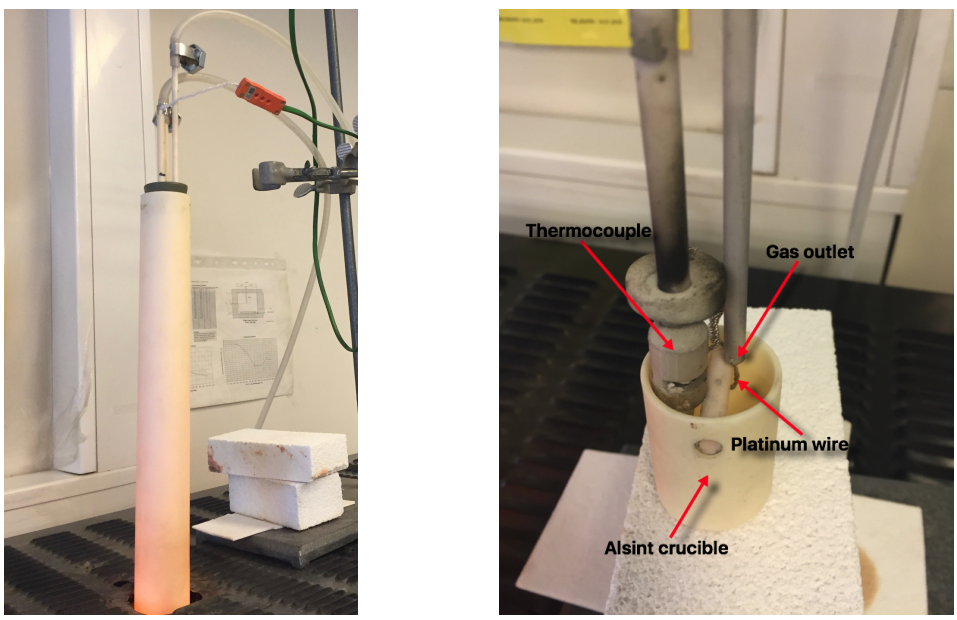

Figure 3.7: Experimental setup for CO experiments.

A leakage test of CO was performed by checking with a mobile CO detector. If no leakage was found, the CO feed was closed, and the sample was flushed with argon. The sample was then lowered into the furnace until it obtained a temperature of about 1000°C. The gas atmosphere was then changed to CO before the sample was lowered further into the furnace by 1 cm every 15th second until it reached 1500°C. This was to get a gradual heating of the equipment. It was then held at the same position for the desired hold time. The sample was then raised by 1 cm every 15th second until the temperature had lowered to 1000°C. The gas atmosphere was then

switched to argon before it was further raised until the temperature was about 200°C. The argon feed was then turned off, and the sample could be raised out of the alsint tube. During heating in CO, the strain was too large on the platinum wire, so it easily broke and the sample was then left at the bottom of the alsint tube. Only one successful experiment was accomplished with this setup after several attempts.

3.5 Wettability experiment

To visually record the heating of a quartz sample, a wettability furnace was used. A quartz sample was prepared for this experiment by drilling out a cylinder with a diameter of 4 mm and then cut to have a height of about 4 mm. Any edges was finally polished away.

The wettability furnace is a closed furnace with graphite heat elements. This allows the possibility for choosing desired gas atmosphere and controlled heating rate. Figure 3.8 shows the furnace setup [2].

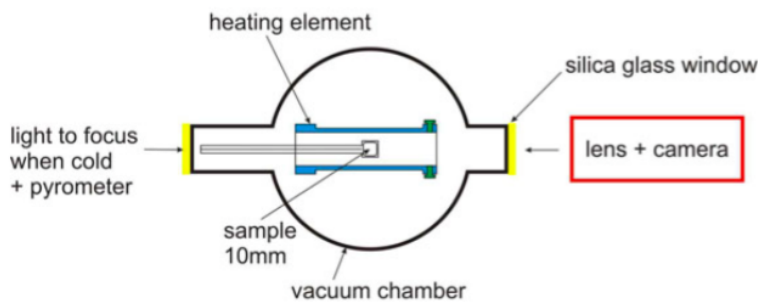

Figure 3.8: Schematic overview of wettability furnace reprinted from [2]

The quartz sample, which also in this experiment was Qz 29, was placed on a graphite substrate with a Mo cap surrounding it. The camera, which is placed outside the furnace, records the sample by taking picture every second and register the temperature at every picture taken. Based on this information, the contact angle between the quartz sample and the graphite substrate can be calculated as a function of time or temperature. By comparing the contact angle at different temperatures, a volume expansion can be calculated.

The sample was investigated with a heating rate of 300°C/min from room temperature to 900°C, 50°C/min to 1200°C and 11°C/min to 1600°C and with no hold time. The contact angle was after this found at 1020, 1500, 1550, 1600 and 1605°C so the volume expansion could be calculated. Since the sample only is about 0.1 g, it is problematic to further investigate the sample with XRD.

3.6 X-ray diffraction

For X-ray diffraction analysis, the grains that were splitted out from the heated and crushed sample, were grinded further to a powder. A boron carbide mortar was used for this until the powder had as little preferred alignment as possible. The sample was prepared in a backloading sample holder. The quantification of amorphous phase requires an addition of a standard material. The internal standard method was used for this. Here, the standard material, which in these experiments has been corundum, Al_2O_3, is added to the sample with a known, accurate ratio. This is done by weighing out the amount of quartz sample and the amount of standard material and calculate the percentage of standard material. The added amount of standard material should be approximately 30 % of the sample and after the analysis, the phases in the quartz sample were normalized accordingly. The software DIFFRAC^{TOPAS} is used to analyze and measure the phases present in the sample and calculate the amount of amorphous phase in the samples. The XRD instrument used, was a Bruker D8 advance called DaVinci-1, placed in Kjemiblokk 2, NTNU.

3.7 Light microscope

A light microscope was used to investigate one particle that had been heat treated and one that has not, to see if any differences could be found. Sample 19, which has been heated for 20 minutes at 1600°C, was used for this investigation. The particle was cut in two to get a flat surface in the center of the particle. It was then cut into a smaller piece, to easily cast it in epoxy. The particle was investigated in a Reichert MeF3 A light microscope. The magnification used was 10x1, so a magnification of 100x was obtained. A few captions of each sample were finally taken.

Chapter 4

Results

4.1 Conversion of quartz samples

Samples of 50 grams and 100 grams was heated for 30 and 40 minutes at 1600°C. This was an extension to experiments done in previous project work [15]. It was seen that experiments with a longer hold time than in the previous experiments, could be found interesting. The results from this can be seen in table 4.1. This shows that there still is just a small amount of cristobalite. It is found a large amount of quartz, but it is seen that the conversion to amorphous phase is relatively fast regardless of the size of the particle. It does although show a smaller conversion rate of quartz for the particles of 100 grams than the particles of 50 grams.

Sample 4 was first found to have an extremely small conversion compared to the other samples. Two XRD analysis were done on the sample, but both showed approximately the same results. A new particle was heated with the same program to see if the same results was obtained. The table shows that it was not found the same results. The second parallel of sample 4 gave results that were more comparable to the rest of the results.

A few other samples gave results that seemed to be diverging, so these samples were run in an extra parallel. To investigate this deviation, three parallels of sample 3 were run. These parallels gave a deviation of about ±10 % for the converted amount. This is thus the deviation for quartz and amorphous phase, since the sample contains mostly these phases. The amount of cristobalite is not found to vary much and shows a deviation of about ±1 %. This is although a large deviation compared

Table 4.1: Results for heated quartz samples heated to 1600°C for particles of 50 grams and 100 grams of Qz29 from Faleq.

Sample	**Mass [g]**	**Hold Time [min]**	**Cristobalite [%]**	**Quartz [%]**	**Amorphous phase [%]**
1	50	30	2.05	47.2	50.8
2	50	40	5.61	39.1	55.3
3-1	100	30	1.75	58.8	39.5
3-2	100	30	2.49	41.05	56.49
3-3	100	30	1.00	51.33	47.67
4-1	100	40	0.03	98.57	1.40
4-2	100	40	0.02	98.9	1.13
4-3	100	40	6.26	33.18	60.56
21	50	10	0.09	68.35	31.54

to the amount of cristobalite, which here is about 50 % of the total cristobalite amount.

The same type of samples were also investigated at 1700°C. The samples was also here 50 and 100 grams. These results show a faster conversion rate than the samples heated to 1600°C as seen in table 4.2.

Table 4.2: Results for quartz samples of Qz29, Faleq, heated to 1700°C.

Sample	**Mass [g]**	**Hold time [min]**	**Cristobalite [%]**	**Quartz [%]**	**Amorphous phase [%]**
5	50	0	1.14	48.4	50.5
6	50	10	3.17	13.6	83.2
7	50	20	6.35	1.45	92.2
8	50	30	6.92	0.763	92.3
9-1	50	40	21.3	0	78.7
9-2	50	40	6.29	0	93.71
10	100	0	0.811	51.5	47.7
11-1	100	0	1.65	77.68	20.67
11-2	100	10	1.51	74.7	23.8
11-3	100	10	0.14	55.85	44.02
12	100	20	4.10	32.0	63.9
13	100	30	4.54	5.54	89.9
14	100	40	5.09	0.726	94.2

These results can be seen graphically in figure 4.1 where the amount of phases is plotted against hold time. As seen from the figure and the table, the conversion rate is similar for the samples heated with no hold time. The additional data points in the diagram are other parallels of the same treatment. Some of these results are considered as deviating.

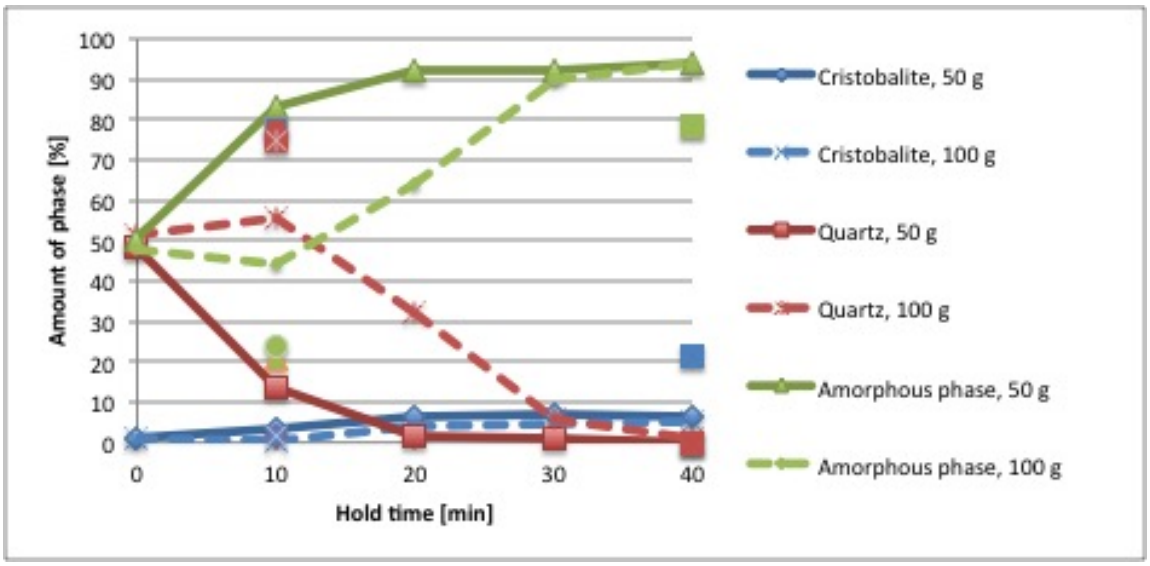

Figure 4.1: The amount of phases in samples of Qz29, Faleq, heated to 1700°C as a function of hold time.

The transition rate to amorphous phase is slower for the particle of 100 grams than for the particle of 50 grams, but the rate of transition to cristobalite is similar for both sizes. It is although found that the transition to amorphous phase generally is fast. Without hold time, just heating to 1700°C, there is already a conversion of about 50 % for both sizes of particles. The transition to cristobalite is found to be slow also at a temperature of 1700°C. After 40 minutes hold time, the conversion has reached 100 % for the particles of 50 grams and nearly 100 % for 100 grams. The particle contains although mostly amorphous phase, up to 94 %, because of the slow transition to cristobalite. A second parallel was run for both sample 9 and sample 11. In addition, was a second XRD analysis performed on the first parallel of sample 11. The first parallel of the samples are annotated 9-1 and 11-1, the second XRD analysis on the first parallel of sample 11 is annotated 11-2 and the second parallel of sample 11 is annotated 11-3. The second parallel of sample 9 is annotated 9-2.

To investigate the effect of size, samples with larger size difference, 10 grams and

200 grams, were investigated. Results can be seen in table 4.3. It was not found any distinct size effect between the samples of 10 grams and the samples of 200 grams.

Table 4.3: Results for quartz samples of Qz29, Faleq, heated at 1600°C for sizes of 10 grams and 200 grams.

Sample	**Mass [g]**	**Hold time [min]**	**Cristobalite [%]**	**Quartz [%]**	**Amorphous phase [%]**
15	10	0	0.02	84.5	15.5
16	10	20	0.38	74.2	25.4
17	10	40	5.07	51.6	43.2
18	200	0	0	80.10	19.90
19-1	200	20	0.03	88.90	11.07
19-2	200	20	0.54	65.22	34.25
19-3	200	20	0.65	65.14	34.21
20	200	40	3.00	39.33	57.66

When comparing how much has been converted for the different hold times in the two sizes at 1600°C, the results are similar. This can be seen in figure 4.2. It is in fact here found that most of the samples of 200 grams is more converted than the samples of 10 grams. This is although within the range of variation. With no hold time, the samples have approximately the same conversion rate. Sample 19-1 showed low conversion compared to the other samples analyzed, and a second parallel was run for the sample, to investigate if the first parallel was an outlier. It was performed a second XRD analysis, that resulted in what is referred to as sample 19-2 and 19-3 in the table. These results correlated better with the other results and they were coinciding well with each other, making it seem as if the XRD analysis is accurate. In the figures including sample 19, an average of sample 19-2 and 19-3 is used. Sample 19-1 is considered an outlier and is not used for other than uncertainty considerations.

After 40 minutes heating, the samples investigated vary in terms of the amount of quartz has been converted to amorphous phase. The main factor for different conversion amounts, are the temperature the sample has been heated to. This can be seen in figure 4.3. The amount of cristobalite is, as seen in the figure, small and similar for all samples investigated.

The most converted sample, sample 9, which has been heated for 40 minutes at 1700°C, contains no quartz. The sample of 50 grams has converted to a glassy phase

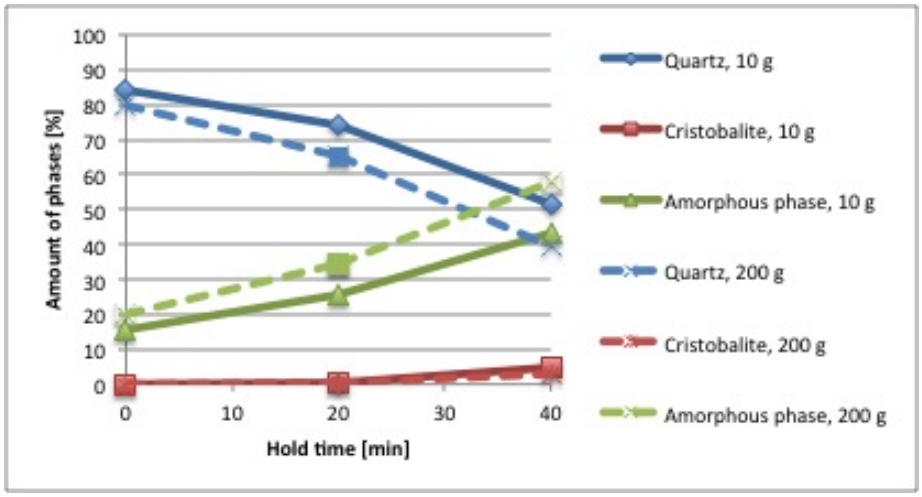

Figure 4.2: The amount of phases in samples of 10 grams and 200 grams of the quartz type Qz29, Faleq, heated to 1600°C.

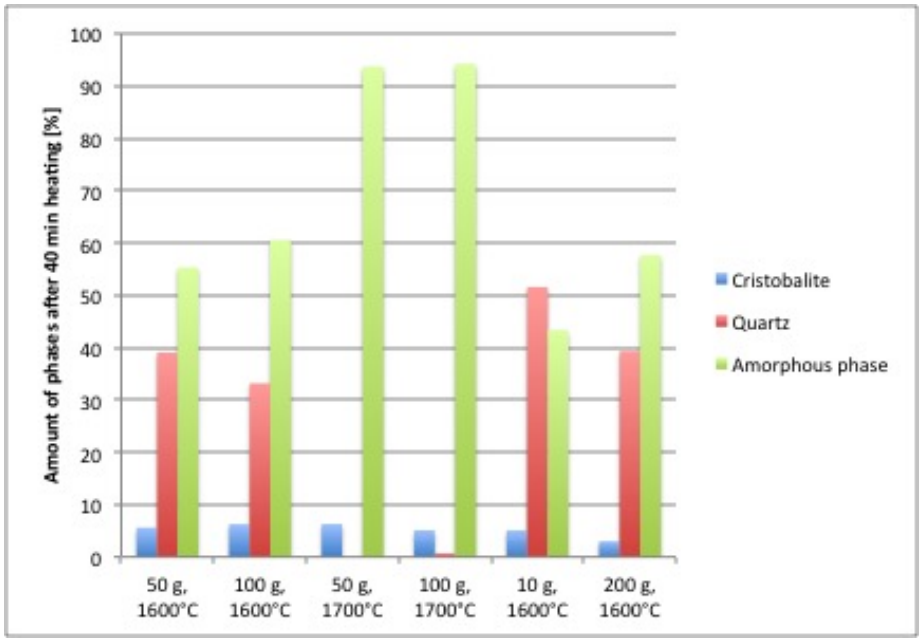

Figure 4.3: The amount of phases in samples of different sizes of quartz type Qz29, Faleq, heated 40 minutes at 1600°C and 1700°C.

in the center of the particle, as seen in figure 4.4 . Based on the XRD analysis, which

found that it contains 93.7 % amorphous phase and the rest is cristobalite, there is almost no crystalline state of the sample left, or it has not yet been created.

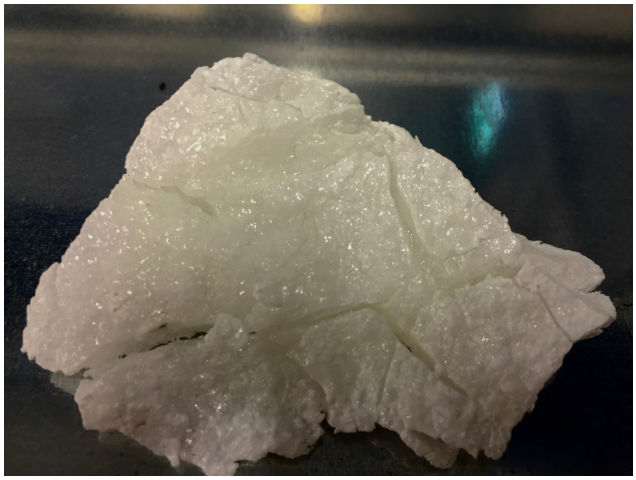

Figure 4.4: The most converted sample, sample 9, 50 grams particle heated for 40 minutes at 1700°C.

4.2 Analyzed samples from furnace excavation

Three unreacted, but heat exposed quartz samples that was taken out at a furnace excavation in Wacker's plant at Holla was analyzed with XRD. The results is shown in table 4.4.

In sample 2 and 3, it is found quite a large difference in phases between the edge and the center of the sample. It is although not found a size effect when comparing where in the particle the sample analyzed has been taken from and the amount of quartz converted. In sample 1 and 2, the samples from the center are more reacted than the ones at the edge. In sample 3 it is the opposite, but the difference is small. This rules out any size effects of these samples. It is found a slow conversion rate of these samples with a maximum converted amount of 25 %. When looking at where in the furnace the samples were obtained, sample 3 was found closest to the electrode, with sample 2 close by. Sample 1 was found about one meter further away from the electrode. This coincide well with the results where sample 3 is the most converted, and sample 2 is silimar, but a little less converted. Sample 1 is about 10 % less

Table 4.4: Overview of phases in samples obtained in excavation of a Holla furnace.

Sample 1	**Center**	**Edge**	**Average**
Cristobalite	0.02	0	0.01
Quartz	89.62	91.76	90.69
Amorphous phase	10.36	8.24	9.30
Sample 2	**Center**	**Edge**	**Average**
Cristobalite	0.05	0.27	0.16
Quartz	79.41	88.36	83.89
Amorphous phase	20.55	11.37	15.96
Sample 3	**Center**	**Edge**	**Average**
Cristobalite	0.61	0.16	0.385
Quartz	86.10	74.73	80.42
Amorphous phase	13.29	25.10	19.20

converted than the other two samples. It could however be different types of quartz, and this could therefore affect the conversion.

4.3 Volume expansion investigations

An experiment was conducted in a wettability furnace to study visual changes in quartz during heating and to calculate the volume expansion after heating. The sample could be seen before and after heating in figure 4.5. No apparent visual changes can be seen in these picures.

It could although be found an increase in volume of the sample, calculated by the contact angle between the sample and the graphite layer that the sample is placed on. The volume change as a function of temperature can be seen in figure 4.6 and is found to increase up to almost 10 % during heating to 1600°C with no hold time. The volume expansion happens particularly when the temperature exceeds 1550°C.

When comparing a particle that has been heated to 1600°C and a particle that has not been heated, it can be seen a remarkable volume expansion of the particle. This can be seen in figure 4.7. Here, the heights of the particles are approximately equal, but the heat treated sample is much larger.

The heat treated sample shown here is sample 20, which is a particle of 200 grams heated to 1600°C for 40 minutes. The heat treated particle is additionally porous

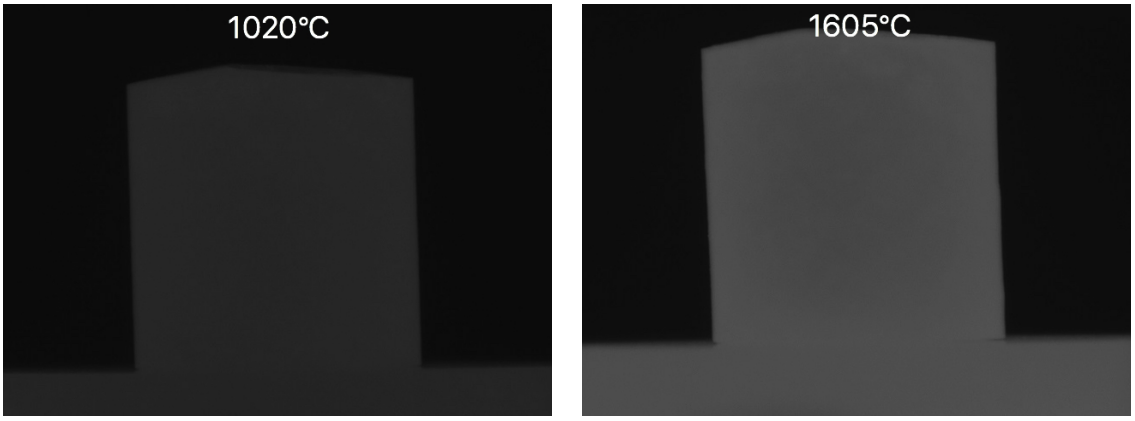

Figure 4.5: Quartz, Qz29 (Faleq), during heating in wettability furnace.

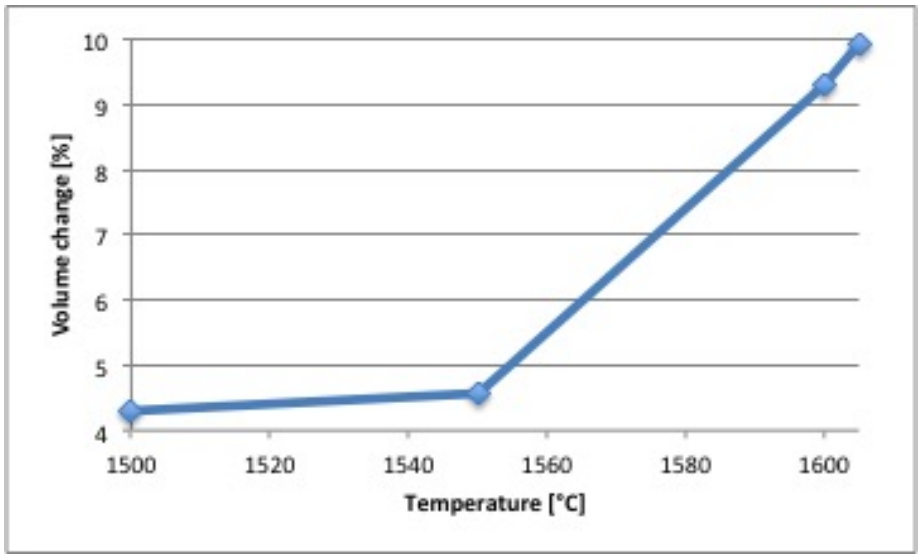

Figure 4.6: The volume change during heating in wettability furnace as a function of temperature.

and brittle. It has, however, not fallen apart.

Figure 4.7: One heated sample to the left and one sample that is not heated to the right. Both samples are about 200 grams.

4.4 Light microscopy

One heat treated sample and one sample that has not been heat treated has been studied in a light microscope. The heat treated sample was sample 19-1, which has been heated to 1600°C for 20 minutes. Figure 4.8a and 4.8b are pictures of the heat treated sample with 100x magnification. Figure 4.8c and 4.8d are pictures of the untreated sample. No distinct difference is found in the pictures of the two different samples. It could although be found some small brighter areas in the sample that was heat treated. The black areas are due to uneven surface, and are cavities.

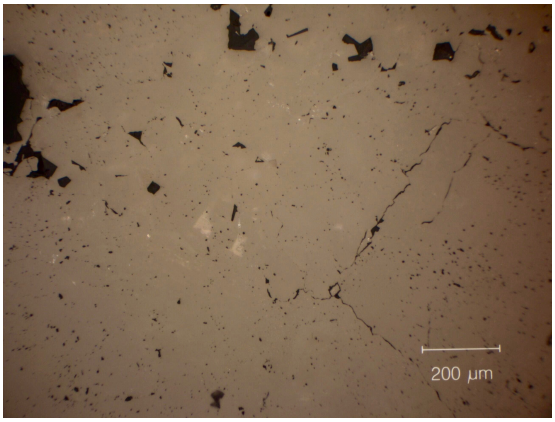

(a) Heat treated

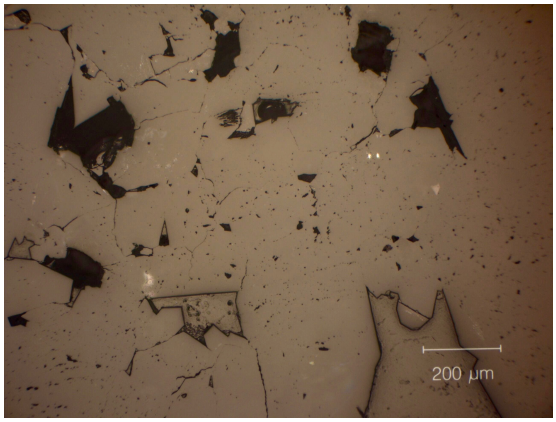

(b) Heat treated

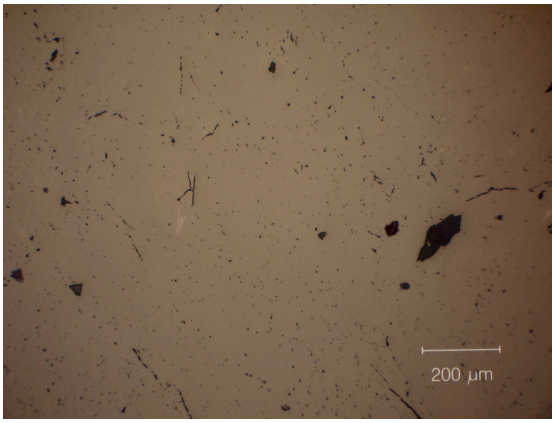

(c) Untreated

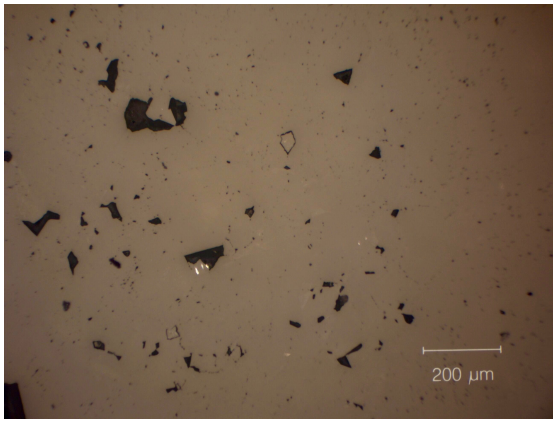

(d) Untreated

Figure 4.8: Samples of quartz (Qz29, Faleq) investigated in light microscope. Sample 4.8a and 4.8b are heat treated at 1600°C for 20 minutes, while sample 4.8c and 4.8d are untreated.

Chapter 5

Discussion

5.1 Conversion of β-quartz to β-cristobalite

The conversion rate of one quartz type, Qz 29 from Faleq, has been studied with sizes of 50 grams and 100 grams to 1600°C both in this study and a previous study [15]. Figure 5.1 shows these results combined, so a complete data series can be studied.

The transformation to amorphous phase and cristobalite seems independent of the size. The maximum difference between the two sizes for the same hold time, is here found to be 12 %. Three different parallels of sample 3 were heat treated according to the same procedure, and it was found a difference of more than 17 % quartz between the most and least converted parallel. It could therefore be said that it is not found a size effect here, but it could neither be ruled out according to the deviation of the results. It can also from these results be said that the transformation to amorphous phase is fast, but the transition to cristobalite is slow.

To study the size effect of a quartz particle, samples of four different sizes were investigated. The conversion rate from quartz during heating looks independent of size, as shown in figure 5.2. The particles of 200 grams are converted just as much as the particles of 10 grams.

While it for samples heated to 1600°C is not found any distinct size effect, it could seem as it for samples heated to 1700°C, the size might have an effect. This can be seen in figure 5.3. Here it is seen that the transformation to amorphous phase, which

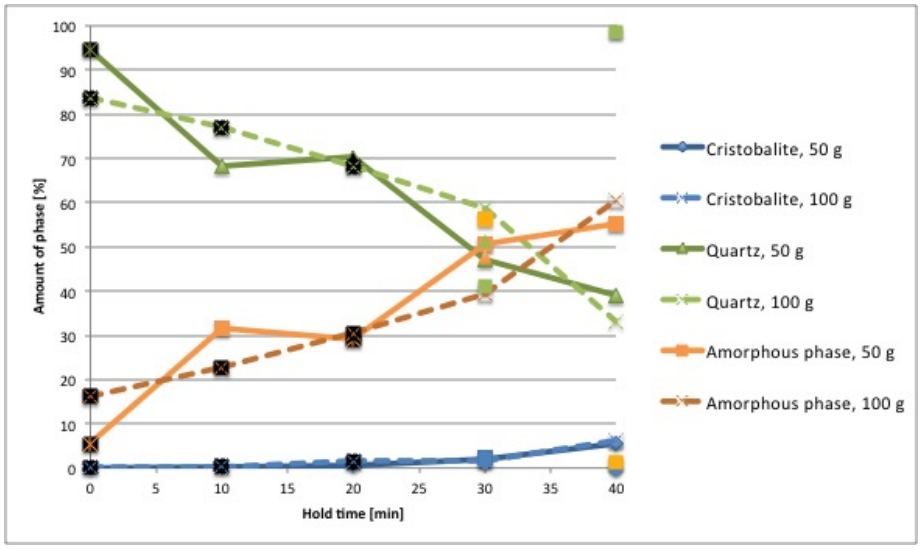

Figure 5.1: The amount of phases in samples of Qz29 (Faleq) heated to 1600°C as a function of hold time. The black data points are from a previous study [15].

.

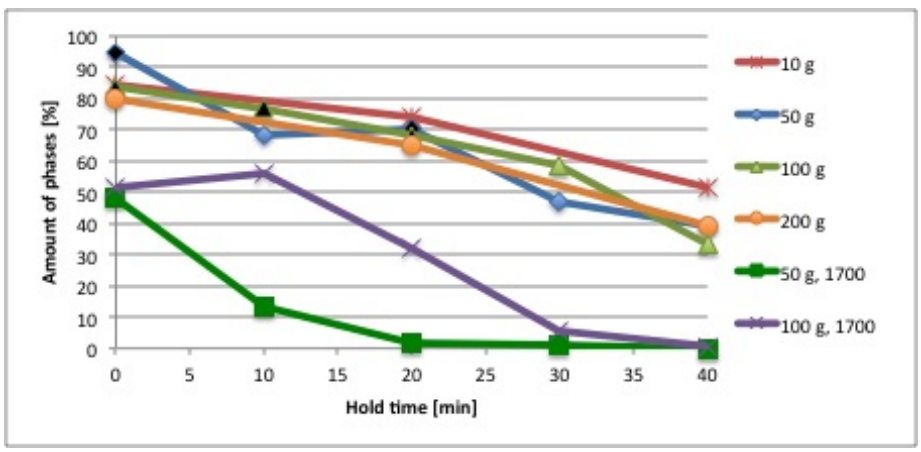

Figure 5.2: The amount of quartz, Qz29 (Faleq), in samples heated to 1600°C and 1700°C as a function of hold time. Black data points are results from previous study [15].

generally is fast, develops slower for 100 grams particles at 1700°C than for particles of 50 grams.

To study the transformation to cristobalite, the amount of cristobalite as a function

of hold time was plotted for the four particle sizes, 10, 50, 100 and 200 grams. This can be seen in figure 5.4. Here it is found that the transformation to cristobalite is similar for all sizes. Only the particle of 200 grams deviated some after 40 minutes. The amount transformed to cristobalite is for all cases very small, and it could easily be seen that the transformation to cristobalite is slow.

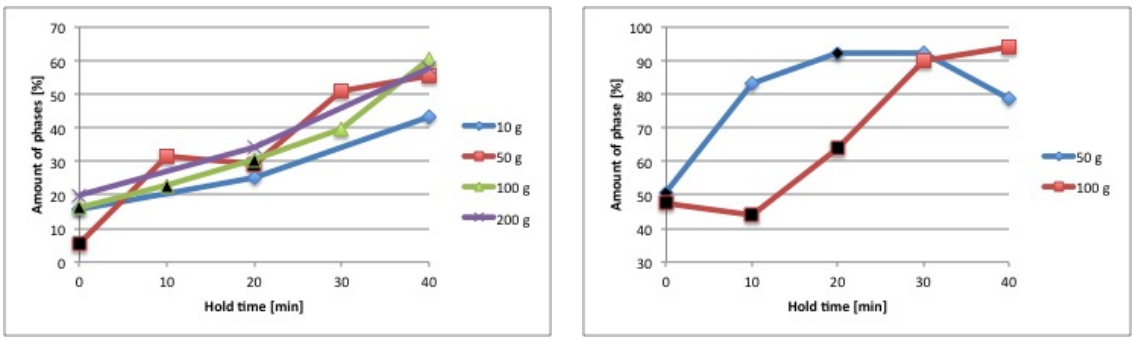

(a) 1600°C (b) 1700°C

Figure 5.3: The amount of amorphous phase in all samples investigated plotted against hold time for the two different temperatures. Black data points are from previous study [15].

The transformation to amorphous phase is rapid at 1700°C and the samples already contain an amount of about 50 % amorphous phase after just heating to 1700°C, which took about 30 minutes, and no hold time. These results support the theory described by Chaklader et al. [21] and Stevens et al. [1] which says that transformation to cristobalite from quartz goes through a transition phase. It is found a clear trend of a fast transition to amorphous phase and a slow transition to cristobalite. Compared to previously tested quartz types [26], Qz29 has an especially slow transition to cristobalite. This can be seen in figure 5.5, where the amount of cristobalite is plotted against hold time for Qz 29 (Faleq) and Qz 9. The data for Qz 9 are from previous studies by Kjelstadli [15].

The highly debated tridymite phase was not studied in the current research, since it previously has been established by studies that tridymite not is a stable phase without presence of impurities [27] [32]. Faleq is a high purity quartz, and tridymite will therefore most likely be an unstable phase and not important for this study.

It was stated by Wiik [17] that the conversion from quartz to amorphous phase is a phase boundary process that follows equation 2.39. By using this equation and the theoretical value of radius of the quartz samples, the radial velocity of decomposition

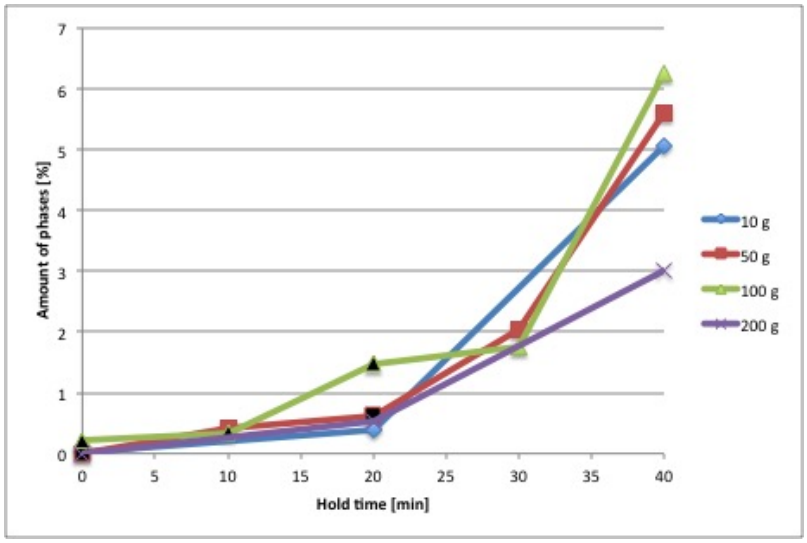

Figure 5.4: The amount of cristobalite in samples for quartz type Qz29 (Faleq), heated to 1600°C as a function of hold time. The samples investigated is of four different particle sizes. Black data points are from previous study [15].

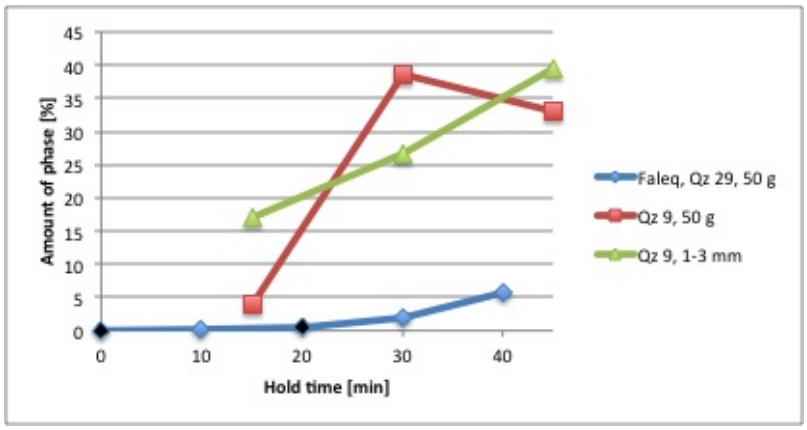

Figure 5.5: The amount of cristobalite in samples heated to 1600°C as a function of hold time. The Qz9 data series and black data points are from previous studies [15].

could be calculated. The calculated values can be seen plotted against hold time in figure 5.6. It is found that for the different sizes of samples heated to 1600°C, the radial velocity is highest for the largest samples of 200 grams and lowest for the smallest samples of 10 grams. This is because the largest samples are converted by the same rate as the smallest sample, and the 200 grams sample will then in reality

have more transformed mass and higher velocity. It could from this be argued that it is not rate limiting to have a larger sample, than to have a smaller sample. In the samples heated to 1700°C a different trend is found. The radial velocity is for the largest samples found to be remarkably lower in the beginning of the hold time. From this it could be argued that the size effect is larger at higher temperatures. The reason for this could be that the thermal distribution in quartz might be slower than the heating rate to 1700°C that the sample is exposed to in these experiments. It could although seem as this evens out at a longer hold time.

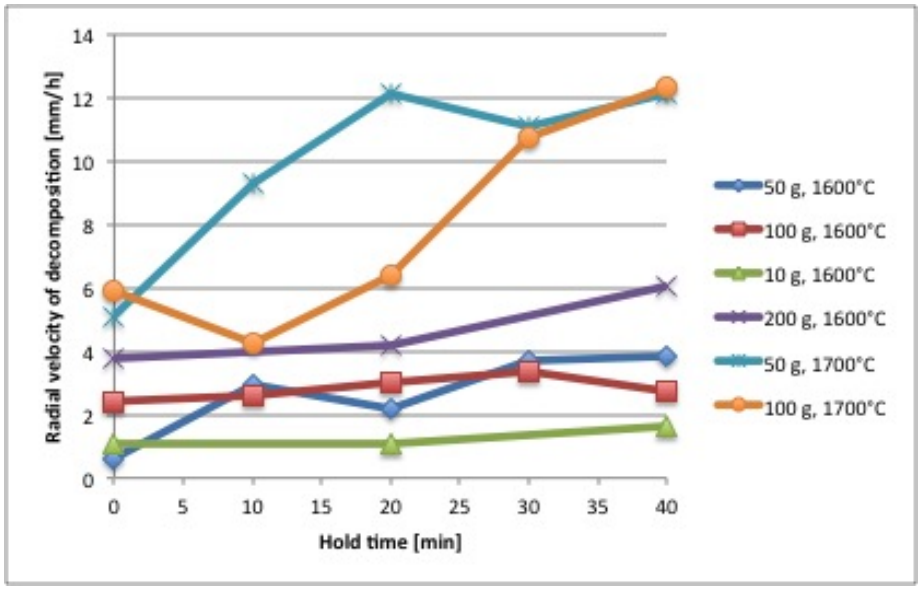

Figure 5.6: The calculated value of radial velocity in Qz29 (Faleq), calculated from eq. 2.39, plotted against hold time.

When the sample is heated, the thermal distribution occurs by the shrinking core model. Thus, the heat transfers from the outside and in towards the center. As shown in figure 3.6, there is a small difference in how fast a particle is heated through depending how large the particle is. It takes about 25 minutes before a 100 grams particle is heated through at 1600°C and about 30 minutes at 1700°C. These all depend on the size of the particle, of course. These differences could therefore give a certain size effect because of rate limitations in the thermal diffusion. In the simulation it is used a thermal diffusivity value of 0.75 mm^2/s. This value is the calculated thermal diffusivity value for β-quartz. It is in the simulation assumed a constant thermal diffusivity value even at high temperatures, where the particle

has been transformed into different phases. The thermal diffusivity value for β-cristobalite and amorphous phase is not known and could affect the heating rate of the particle.

The mechanism of the phase transformation is more uncertain. The transformation requires only heat diffusion, and no mass diffusion. There is nothing, such as off-gases, to be transported out during the transformation. This makes it possible that the transformations could occur by nucleation mechanism. If the transformation occurred by shrinking core, it should be possible to see a size effect for the transition, and not just one that seem to be limited by heat diffusion. Rosenqvist [7] described that for the shrinking core model, when a reaction increase the volume of the reaction product it creates a dense layer. The diffusion will then take place through the crystal lattice. If the phase transformations in quartz transformed according to the shrinking core mechanism, it should be possible to see such a dense layer boundary due to the volume increase in the phase transformations. Especially for the samples from the furnace excavation, it should be found a difference in conversion between the center and the edge of the sample. This is because of the sharp boundary between reacted and unreacted phase that should be found for the shrinking core model. Since it is here found a larger conversion in the center than at the edge in some of the samples, it is reasonable to assume that the conversion from quartz occurs by nucleation. It could seem as if the transformation to cristobalite in this case still only is in the nucleation phase, and has not started to propagate much because of the low concentrations of cristobalite. As Mitra [23] suggested, the conversion of quartz to transition phase is boundary-controlled, and conversion from transition phase to cristobalite is concentration-controlled. The latter suggestion could be an explanation to the results found here, where is it expected absence of cristobalite until enough amorphous phase is produced for enabling cristobalite formation.

The variation in degree of conversion between samples after the same heat treatment may be a result of impurities that catalyze or inhibit the conversion. Faleq is a high purity quartz, but because of the large differences and deviations in similar samples, this would be a reasonable assumption.

In sample 9 it was seen a glassy surface on the particle after heating. In the XRD analysis it was found that the particle had been completely converted during the heat treatment. It was found 93 % amorphous phase in the analysis. It could be debated if this is the intermediate phase between quartz and cristobalite, or if the sample has started softening/melting. Since it previously has been found melted quartz in experiments heated to 1700°C [14], it is possible that the sample has started melting, and will continue melting if the sample is heated for a longer time.

It will in that case not transform into cristobalite. As described by Presser [10], the crystallization rate of amorphous silica toward β-cristobalite reaches a maximum at 1677°C. At temperatures higher than this, the silica layer becomes more fluid and the β-cristobalite grain boundaries will be closed. This could be the case for the samples heated to 1700°C. It is in those samples found a large amount of amorphous phase and very little amount of cristobalite. It also coincide well with what has been seen for sample 9. This could have an impact on the silicon process, since it skips a phase transformation and the time before the particle starts to melt decreases.

In the samples investigated in light microscope, it was hard to see any distinct differences between the samples heat treated and the samples that had not been heat treated. When the heat treated sample investigated in light microscope later was analyzed in XRD, it was found that the sample was hardly converted. It could although be found some small brighter spots in the pictures of the treated sample. What these spots indicates is not known, but they are randomly placed in the samples. This could argue for a nucleation mechanism of the starting phase transformations.

It was described by Aasly [6] in the theory that quartz has an average retention time of 5.7 hours. It is here likely that the particle has a smaller heating gradient than the particles heated in current experiments. The limitations of heat transportation should therefore not be a problem during the silicon process.

5.2 Investigated samples from furnace excavation

The samples obtained from a furnace excavation at Wacker's Holla plant, were found at different distances from the electrodes. Sample 3 was found closest to electrode 1, with sample 2 just beside. Sample 1 was furthest away from the electrode, about 1 meter further out. This corresponds well with the analysis done on the samples. Sample 3 is the most converted sample, containing an average of 80.42 % quartz. Sample 2 has a similar average, with 83.89 % quartz, while sample 1 is clearly less converted with 90.69 % quartz. The quartz types used in the furnace was from Faleq, Tana and Erimsa. In a previous study by Kjelstadli [15], several quartz types was tested. The results from this study can be seen in figure 2.14. This study shows a faster transformation to cristobalite for some quartz types than what is found for the quartz type in the current study, Qz29, which also can be seen in figure 5.5. The samples from the furnace excavation show approximately no cristobalite. It could be advocated that the temperature not has exceeded the transition temperature for cristobalite at 1470°C. It should in that case around this temperature contain an

amount of cristobalite of significance. It was neither expected, based on where in the furnace the samples were taken from, that the sample had been exposed to such a temperature. It is although said by Presser et al. [10] that β-cristobalite formation takes place after about 20 hours between 1100°C and 1200°C, so it could indicate that the furnace has been at around this temperature. The amount of amorphous phase is found to be up to 25 % in the sample laying closest to the electrode. It is said in the theory by Stevens et al. [1] that the transition temperature for the transition phase is at 1300°C. It is also said by Wu et al. [33] that amorphous phase is found at 800°C in small grained quartz. It was although not found at neither 900°C or 1000°C for large grained samples (50 and 80 nm). This is thus not a properly established transition temperature, so it does not necessarily mean that the temperature has reached 1300°C in the environment around the sample, even though the particles contain amorphous phase. Since it also previously has been found cristobalite in samples after 20 hours of heating between 1100°C and 1200°C, amorphous phase must have been formed in advance of this. Thus, it is from the analyze of which phases the quartz particles contain, not possible decide the temperature they have been exposed to in the furnace.

5.3 Volume expansion

During the wettability experiment it was found a volume expansion of almost 10 %. From the literature it is known that cristobalite should have a volume expansion of 17 % when transforming from quartz [5]. The amount of cristobalite in the sample heated in the wettability furnace is not known. It could although be expected to be small. In the samples heated to 1600°C that has been analyzed in XRD, a maximum of 5.6 % cristobalite was found. If the volume expansion in the wettability furnace was caused by the transformation to cristobalite alone, the sample should contain almost 60 % cristobalite. The heating rate was in this experiment much lower than the heating rate of the samples analyzed in XRD. It is although reasonable to think that the amount of cristobalite would not be this large. This could also be supported by previous results from BET investigations [15]. When comparing the results for the 50 grams Qz29 particle, it is found an increase of surface area of 46 % between the samples that was heated for 0 and 20 minutes. For the particle of 100 grams, a surface area increase of 26 % was found. The surface area : volume ratio would in any case of geometry give a larger increase of volume than the increase of amount of cristobalite. Because of these data, it would be reasonable to assume that there are several factors that increase the volume of quartz during heating.

In figure 4.7 it is seen a reacted and unreacted sample. The reacted sample was sample 20, heated for 40 minutes at 1600°C. In the XRD analysis it is found a transformation to cristobalite of 3 %. If the volume change only was caused by the transformation to cristobalite, the volume increase should only be 0.51 %. Figure 4.7 shows a much larger volume increase than this. Taking the amorphous phase into consideration, which is found to be 58 %, it is expected that this phase could cause in a significant volume expansion.

Presser et al. [10] said that the density in amorphous phase and β-cristobalite is similar, $\rho = 2000 - 2200$ kg/m^3 and 2200 kg/m^3, respectively. It should therefore cause a volume expansion of about the same value, and even a little larger, during heating. Wiik [17] claimed that the amorphous phase has a much lower density compared with quartz and would therefore occupy a greater volume than quartz. This would result in tension in form of cracks. It was in the same study found that large amounts of amorphous phase with no cristobalite looked opaque white and crumbled easily to powder. This correlates well with the current study. The heat treated sample shown in figure 4.7 is opaque white and crumbled easily into powder by hitting it with small force. Since this sample contained almost 60 % amorphous phase it is possibly highly fragmented because it goes through a reconstructive transformation by breaking the Si-O bonds, since one third of the bonds must be broken and reformed [1]. It is therefore a possibility that a large number of homogeneously distributed internal nucleation centers would be available so that nucleation and growth of cristobalite would occur throughout the volume of the transition phase instead of being localized on the outer surface, like it is described by Wiik [17].

The cristobalite $\alpha - \beta$ inversion described by Presser et al. [10] should give a volume decrease of 6.2 vol% and give a crack formation. This is hard to visually see since the sample already has crack formation because of a large volume expansion during heating. The sample was examined during cooling before and after the sample reached 270°C, and the volume decrease was not seen with the naked eye. The volume decrease during cooling was not studied in the wettability furnace.

5.4 Evaluation of experimental setup

5.4.1 Heating of quartz

The temperature in the furnace was logged during heating for some samples. A logging of specific samples was only obtained in the original furnace. In the replacement furnace a logging method was not found before the experiments were finished. It was therefore only obtained one logging for each temperature in this furnace. The logging of the original furnace showed a stable, consistent heating for both temperatures. The temperature in both the center of the furnace and in the furnace wall was logged. The temperature in the furnace wall is more continuous than in the center. The thermocouple in the center is although placed in an alsint tube and is therefore shadowed from heat radiation. It is of course more exposed to heat radiation than the thermocouple in the wall, but not as exposed as the sample is. The logging of the replacement furnace (figure 3.4), showed a similar curve as for the original furnace. It should therefore not be a significant source of deviation for the results.

A temperature profile in the Nabertherm furnace was made by moving the alsint tube downwards in the furnace. The temperature profile can be seen in figure 3.5. The samples are maximum 5 cm in height, and the temperature difference from the bottom to 5 cm is measured to be about 5°C. This is although the difference inside the alsint tube, and it could therefore possibly be larger than measured. It is however not thought to be a difference that is large enough to have an impact on the results.

5.4.2 Experiments in CO atmosphere

It was attempted to perform heating experiments of quartz in CO atmosphere. This gives rise to a challenge due to safety regarding CO gas. A completely closed system must be created to avoid leakage to the environment. As shown in figure 3.7 this was done by using a tube closed by a plug with holes for different rods, one for a gas inlet, one for gas outlet and one for a thermocouple. A crucible containing the sample was attached to the thermocouple by a platinum wire. This platinum wire gave rise to the problems for this experimental setup. During heating, this platinum wire breaks. It was first attempted to heat the sample to 1600°C, but the wire broke every time. It was then attempted to lower the temperature to 1500°C. After a few attempts, the experiment was successful with a hold time of 30 minutes. To get a

basis for comparison, it was attempted to do an experiment with 60 minutes. It was although, after several attempts, not achieved a successful experiment.

After several unsuccessful experiments, this setup was not continued. Since there was only one successful experiment, without any basis for comparison, it was not included in this report.

This experimental setup has been used successfully in a previous research. It was although in this research not used CO atmosphere, but the same temperature of 1500°C was used. It is thought that the CO atmosphere could have a weakening effect on the platium wire, and an alternative setup should be considered for further research.

5.5 Uncertainty

Three parallels of the same experiment, sample 3, were investigated. Parallel 1 was heated in the original furnace, Nabertherm, and the two next parallels were heated in the replacement furnace, Entech. The change of furnace should not have large impact on the uncertainty of the results since the heating program of the replacement furnace is customized after the original program. It could although give some degree of deviation, since it always would be a certain difference in two different furnaces. The three different parallels gave a difference in 17 % from the most converted sample to the least converted sample. It has also been done two parallels of XRD analysis for sample 4, 11 and 19. This showed a much smaller deviation than for two samples heat treated by the same program. This shows that the deviation of the results largely lies in differences in the particles and could be argued with an effect of inhibiting impurities. Two parallels of sample 19 was also investigated with two XRD analysis of each parallel. The first parallel showed very little conversion, and it was thought that is was an outlier. The second parallel was investigated by analyzing two samples to compare the liability of the XRD results. The two XRD analyzes showed a very small deviation with only 0.1 % difference for each phase for the second parallel. The first parallel showed some deviation in the XRD results, but it was still found a small conversion. The first XRD analysis of the first parallel, was probably a failed weighing in the sample preparation, and is considered to be failed experiment.

It is thought that the differences in the different heat treatments not should give any deviation of significance because of consistent results of the temperature logging. It could therefore seem as if the deviation lies in the quartz itself. The analyzing

method is found to have just a very small deviation, and is also considered insignificant compared to the deviation found by investigating two different parallels. It is therefore thought that the deviation lies in differences in the quartz samples. The different properties in the quartz sample could be caused by impurities that enhance or inhibit the phase transformations during heating.

Chapter 6

Conclusions

- β-quartz is rapidly transformed into a transition phase, which is an amorphous phase, before slowly transforming into β-cristobalite during heating to 1600°C and 1700°C.
- Rate limiting factor at 1600°C seems to be the crystallization of amorphous phase to β-cristobalite.
- No size effect was found for samples heated to 1600°C, even with a large size difference of 10 grams versus 200 grams.
- At 1700°C the thermal diffusion in the particle could be a rate limiting factor in addition to the transition to β-cristobalite. This gives a size effect of the particles because of slower transition in larger particles if the temperature gradient in the process is large.
- Since it is not found any size effect of the phase transition, it is concluded from these results that the mechanism for phase transformations from β-quartz to β-cristobalite is by nucleation.
- It is observed slow transformation to β-cristobalite and indication of melting at 1700°C could support the theory of closed cristobalite grain boundaries at temperatures around 1700°C.
- It is observed large volume expansion during heating. In samples investigated in these experiments, volume expansion is due to low density of the amorphous phase.

- Not much could be seen from the light microscope images taken in these experiments. For visual investigation of the mechanism of phase transformations, it should be prepared a thin layer sample for further investigations.
- No visual change was seen for a sample heated in the wettability furnace, except a volume expansion calculated to be 9.94 %.
- The phase transformation from β-cristobalite to α-cristobalite did not give a volume decrease that was visually observed.

References

[1] S. J. Stevens, R. J. Hand, and J. H. Sharp. The polymorphism of silica. *Journal of Materials Science*, 32:2929–35, 1997.

[2] V. Andersen. Reaction mechanism and kinetics of the high temperature reactions in the silicon process. Master's thesis, NTNU, 2010.

[3] E. Ringdalen. Changes in quartz during heating and the possible effects on si production. *JOM*, 2014.

[4] H. Tveit A. Schei, J. K. Tuset. *High Silicon Alloys*. Tapir forlag, Trondheim, 1998.

[5] E. Ringdalen. Quartz properties in the silicon production. *Silicon for the Chemical and Solar Industry XII*, 2014.

[6] K. Aasly. *Properties and behavior of quartz for the silicon process*. PhD thesis, NTNU, 2008.

[7] T. Rosenqvist. *Principles of Extractive Metallurgy*. Tapir Academic Press, second edition edition, 2004.

[8] C. J. Geankoplis. *Transport Processes and Separation Process Principles*. Prentice Hall, 2009.

[9] M. Ksiazek, T. Manik, M. Tangstad, and E. Ringdalen. The thermal diffusivity of raw materials for ferromanganese production. *The thirteenth International Ferroalloys Congress*, pages 127–136, June 2013.

[10] V. Presser and K. G. Nickel. Silica on silicon carbide. *Critical Reviews in Solid State and Materials Sciences*, 33:1:1–99, 2008.

[11] W. D. Callister Jr. and D. G. Rethwisch. *Materials Science and Engineering*. ISBN: 978-0-470-50586-1. Wiley, 8th edition, 2011.

[12] A. Muan and E. F. Osborn. Phase equilibria among oxides in steelmaking. *Addison-Wesley, Reading, Mass.*, page 236, 1965.

[13] G. Aylward and T. Findlay. *SI Chemical Data*. John Wiley and Sons Australia, Ltd., 6. edition, 2008.

[14] K. Jusnes. Melting and softening of quartz. Project work, IMT, NTNU, 2015.

[15] M. Kjelstadli. Kinetics and mechanism of phase transformation from quartz to cristobalite. Master's thesis, NTNU, 2015.

[16] P. Hayes. *Treatise on Process Metallurgy*, volume 1. Elsevier, 2014.

[17] K. Wiik. *Kinetics of Reactions Between Silica and Carbon*. PhD thesis, NTNU, 1990.

[18] K. Aasly, T. Malvik, and E. Myrhaug. Heating of quartz and formation of cristobalite. 2007.

[19] M. G. Tucker, D. A. Keen, and M.T. Dove. A detailed structural characterization of quartz on heating through the $\alpha-\beta$ phase transition. *Mineralogical Magazine*, 65(4):489–507, 2001.

[20] C. S. Marians and L. W. Hobbs. Network properties of crystalline polymorphs of silica. *Journal of Non-Crystalline Solids*, 124:242–253, 1990.

[21] A. C. D. Chaklader and A. L. Roberts. Transformation of quartz to cristobalite. *J. Amer. Ceram. Soc.*, 44:35–41, 1961.

[22] H. Schneider and A. Majdic. Kinetics of the quartz-cristobalite transformation in refractory-grade silica materials. *Materials Science Forum*, 7:91–102, 1986.

[23] S. Mitra. *Trans. Brit. Ceram Soc.*, 76:71–74, 1977.

[24] F. J. Kuelmer and T. I. Poe. *J. Amer. Ceram. Soc.*, 47:311, 1964.

[25] M. Ksiazek. *The Thermophysical Properties of Raw Materials for Ferromanganese Production*. PhD thesis, NTNU, 2012.

[26] M. Kjelstadli. Kinetics and mechanism of phase transformation from quartz to cristobalite. 2015.

[27] O. W. Flörke. Strukturanomalien bei tridimyt und cristobalit. *Ber. deut. Keram. Ges.*, 32:369–381, 1955.

[28] O. F. Tuttle and J. L. England. Preliminary report on the system $sio_2 - h_2o$. *Bull. Geol. Soc. Am.*, 66:149–152, 1955.

[29] V. G. Hill and R. Roy. Silica structure studies, vi. on tridymites. *Trans. Brit. Ceram Soc.*, 57:496–510, 1958.

[30] D. M. Roy and R. Roy. Tridymite-cristobalite relations and stable solid solutions. *The American Mineralogist*, 49:952–962, 1964.

[31] S. J. Stevens, R. J. Hand, and J. H. Sharp. The temperature dependence of the cristobalite $\alpha - \beta$ inversion. *Journal of Thermal Analysis*, 49:1409–15, 1997.

[32] L. Pagliari, M. Dapiaggi, A. Pavese, and F. Francescon. A kinetic study of the quartz-cristobalite phase transitions. *Journal of the European Ceramic Society*, 33:3403–10, 2013.

[33] S. Wu, D. Wong, and S. Lu. Size effects on silica polymorphism. *J. Am. Ceram. Soc.*, 85(10):2590–92, 2002.

[34] V. Andersen. Investigation of thermal properties of quartz for the silicon industry under reducing atmosphere. Specialization Project, 2009.

[35] I. C. Madsen, N. V. Y. Scarlett, and A. Kern. Description and survey of methodologies for the determination of amorphous content via x-ray powder diffraction. *Z. Kristallogr*, 226:944–955, 2011.

[36] H. P. Klug and L. E. Alexander. X-ray diffraction procedures: for polycrystalline and amorphous materials. page 966, 1974.

[37] David Barthelmy. Quartz mineral data. http://webmineral.com/data/Quartz.shtml.Vz1tHmPfejI.